An Equivalent Classical Plate Model of Corrugated Structures

Zheng Ye [a], Victor L. Berdichevsky [b], Wenbin Yu [a]

[a] *Utah State University, Logan, Utah 84322*
[b] *Wayne State University, Detroit, Michigan 48202*

Abstract

An equivalent classical plate model of corrugated structures is derived using the variational asymptotic method. Starting from a thin shell theory, we carry out an asymptotic analysis of the strain energy in terms of the smallness of a single corrugation with respect to the characteristic length of macroscopic deformation of the corrugated structure. Without invoking any apriori assumptions, we obtained the complete set of analytical formulas for effective plate stiffnesses valid for both shallow and deep corrugations. These formulas can reproduce the well-known classical plate stiffnesses when the corrugated structure is degenerated to a flat plate. The extension-bending coupling stiffnesses are obtained the first time. The complete set of recovery relations are also derived for recovering the fields within the corrugated structure from the strains obtained in the equivalent plate analysis.

Key words: Corrugated structure; Corrugated plate; Homogenization; Equivalent plate; Variational asymptotic method

1 Introduction

Corrugated structures are one of the most important applied branches of thin shells, which have been widely used in civil, automotive, naval and aerospace engineering, to name only some, diaphragms for sensing elements, fiberboards, folded roofs, container walls, sandwich plate cores, bridge decks, ship panels, etc. [1, 2, 3, 4, 5, 6, 7, 8, 9, 10, 11, 12]. Recently, corrugated structures are also applied for flexible wings or morphing wings [13, 14, 15] due to their unique

Email address: wenbin.yu@usu.edu (Wenbin Yu).
URL: http://www.mae.usu.edu/faculty/wenbin/ (Wenbin Yu).

Preprint submitted to *2 October 2013*

Please cite as: http://dx.doi.org/10.1016/j.ijsolstr.2014.02.025

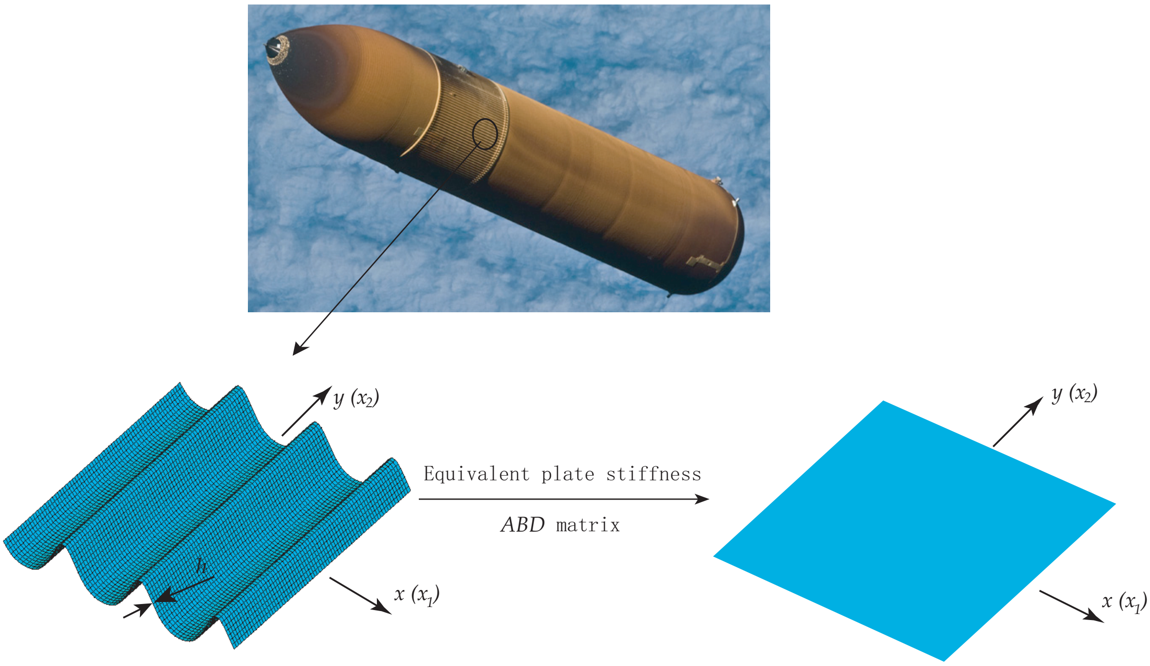

Fig. 1. Equivalent plate modeling of corrugated structures.

characteristics of having orders of magnitude different stiffnesses in different directions.

Although commercial codes such as ANSYS allow one to analyze corrugated structures by meshing all the corrugations with shell elements or solid elements, it is not an efficient or even a practical way to finish prototype in a timely manner as it requires significant computing time, particularly if the structure is formed by hundreds or thousands of corrugations. The common practice in design and analysis of corrugated structures is to model it as an equivalent flat plate, which is possible if the period of corrugation is much smaller than the characteristic length of macroscopic deformation of the structure (see Fig.1). For example, to model the corrugated structure using the Kirchhoff plate model, also called the classical plate model, we need to obtain the following constitutive relations by analyzing a single corrugation:

$$\begin{Bmatrix} N_{xx} \\ N_{yy} \\ N_{xy} \\ M_{xx} \\ M_{yy} \\ M_{xy} \end{Bmatrix} = \begin{bmatrix} A_{11} & A_{12} & 0 & B_{11} & B_{12} & 0 \\ A_{12} & A_{22} & 0 & B_{12} & B_{22} & 0 \\ 0 & 0 & A_{66} & 0 & 0 & B_{66} \\ B_{11} & B_{12} & 0 & D_{11} & D_{12} & 0 \\ B_{12} & B_{22} & 0 & D_{12} & D_{22} & 0 \\ 0 & 0 & B_{66} & 0 & 0 & D_{66} \end{bmatrix} \begin{Bmatrix} \epsilon_{xx} \\ \epsilon_{yy} \\ 2\epsilon_{xy} \\ \kappa_{xx} \\ \kappa_{yy} \\ 2\kappa_{xy} \end{Bmatrix} \equiv \begin{bmatrix} A & B \\ B^T & D \end{bmatrix} \begin{Bmatrix} \epsilon_{xx} \\ \epsilon_{yy} \\ 2\epsilon_{xy} \\ \kappa_{xx} \\ \kappa_{yy} \\ 2\kappa_{xy} \end{Bmatrix} \tag{1}$$

where x, y are the two in-plane coordinates describing the equivalent plate,

Please cite as: http://dx.doi.org/10.1016/j.ijsolstr.2014.02.025

N_{xx}, N_{yy}, N_{xy} the force resultants, M_{xx}, M_{yy}, M_{xy} the moment resultants, ϵ_{xx}, ϵ_{yy}, ϵ_{xy} the membrane strains, $\kappa_{xx}, \kappa_{yy}, \kappa_{xy}$ the curvature strains, A, D and B represent extension stiffnesses, bending stiffnesses, and extension-bending couplings, respectively. The stiffness matrix in Eq. (1) could be in general populated for an equivalent plate model of general corrugated structures. However, it will be shown later that some of the stiffness constants vanish as shown in Eq. (1) for a corrugated structure made of a single isotropic material.

The literature is rich in equivalent plate modeling of corrugated structures with the first treatment known to the authors dated 1923 [16] and a very recent treatment appeared in 2013 [17]. Various methods with different levels of sophistication were used in numerous studies. Generally speaking, existing methods can be generally classified either as engineering approaches based on various assumptions or asymptotic approaches based on asymptotic analysis of governing differential equations of a shell theory. Most methods fall in the category of engineering approaches which invoke various assumptions for boundary conditions and force/moment distribution within the corrugated structure. For a given state of constant strain, the actual (or assumed) distributions of forces and moments within the corrugated structure will be determined. Then force equivalence or energy equivalence is used to derive the corresponding stiffness constants (see [18], [19], [17] and references cited therein). Although both analytical approach and finite element analysis can be used to predict these stiffness constants, the analytical approach has the advantage of providing a set of close-form expressions in terms of the material and geometry characteristics of the corrugated structure while the finite element analysis predicts values which are valid for a specific corrugated structure. Asymptotic approaches exploit the smallness of a single corrugation with respect to characteristic length of macroscopic deformation of the corrugated structure [20, 21, 22, 23]. Substituting asymptotic expansion of the field variables into the governing differential equation of the shell theory, a series of system of governing differential equations corresponding to different orders can be solved to find the relationship between the equivalent plate and the corrugated structure. Because different methods are used to treat this problem, it is not surprising that different results are obtained in previous studies, which will summarized and compared here.

2 Results

To facilitate the comparison of different results in the literature, we need to set up the necessary notations. Let x be the Cartesian coordinate in the corrugation direction and ε the projected length of the corrugation (Fig. 2).

Please cite as: http://dx.doi.org/10.1016/j.ijsolstr.2014.02.025

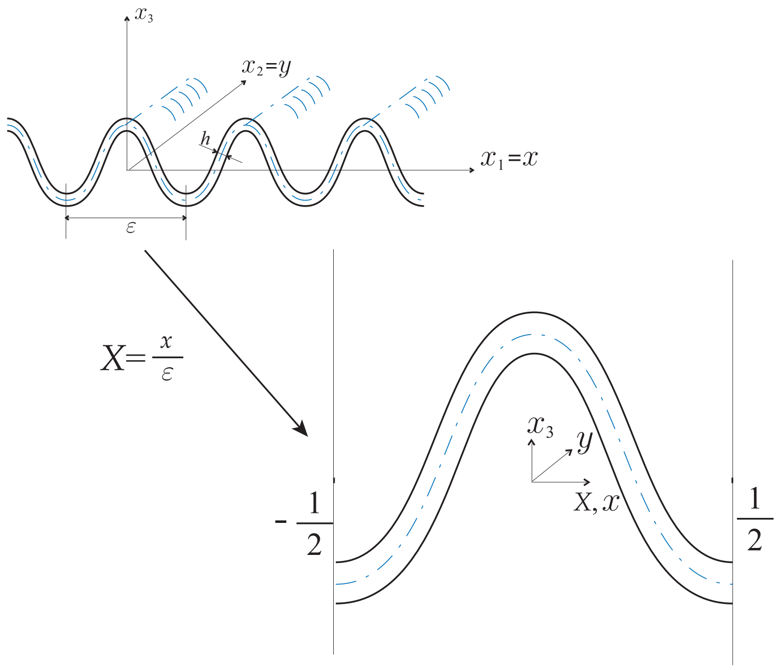

Fig. 2. Shell geometry and unit cell.

We denote by

$$X = \frac{x}{\varepsilon}, \tag{2}$$

the dimensionless "cell coordinate"; Within a cell, X changes between $-1/2$ and $1/2$. For any parameter, f, changing within a cell, $\langle f \rangle$ means the average of the cell,

$$\langle f \rangle \equiv \int_{-\frac{1}{2}}^{\frac{1}{2}} f(X) dX. \tag{3}$$

The shape of the corrugation is described by the $x_3(X)$ which is a periodic function with the period unity. Without loss of generality, one can set

$$\langle x_3 \rangle = 0, \tag{4}$$

by shifting the observer's frame in the vertical direction. Let us also denote

$$x_3 = \varepsilon \phi(X), \tag{5}$$

so that

$$\varphi = \frac{dx_3(x)}{dx} = \frac{d\phi(X)}{dX} \tag{6}$$

Let $a = 1 + \varphi^2$, we can compute the arc-length of the corrugation S and the moment of inertia along the corrugation direction I_y as

$$S = \varepsilon \left\langle \sqrt{a} \right\rangle, \qquad I_y = h\varepsilon^2 \left\langle \phi^2 \sqrt{a} \right\rangle. \tag{7}$$

Please cite as: http://dx.doi.org/10.1016/j.ijsolstr.2014.02.025

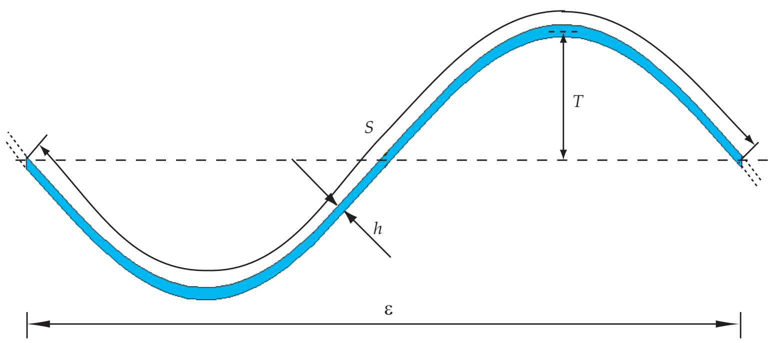

Fig. 3. Unit cell of a corrugated structure (sinusoidal shape is used for illustration).

2.1 Main results from previous studies

To our best knowledge, all existing studies conveniently assume there are no extension-bending couplings, which implies that bending problem can be solved by the following fourth-order partial differential equation:

$$D_{11}\frac{\partial^4 w}{\partial x^4} + 2H\frac{\partial^4 w}{\partial x^2 \partial y^2} + D_{22}\frac{\partial^4 w}{\partial y^4} = p, \tag{8}$$

where x, y are the Cartesian coordinates on the effective plate (Fig.1), w the transverse displacement, p the effective pressure load, $H = D_{12} + 2D_{66}$. Seydel [24] followed Huber [16] and obtained the following formulas for the equivalent bending stiffnesses

$$\begin{aligned} D_{11} &= \frac{\varepsilon}{S}\frac{Eh^3}{12(1-\nu^2)}, \qquad D_{12} = 0, \\ D_{22} &= EI_y, \qquad D_{66} = \frac{S}{\varepsilon}\frac{Eh^3}{24(1+\nu)}. \end{aligned} \tag{9}$$

Here S denotes the arc-length of the corrugation, ε the projected length of the corrugation, I_y the moment of inertia along the corrugation direction, h the thickness (Fig. 3). It is assumed that the corrugated plate is made of isotropic elastic material with the Young's modulus E, and the Poisson's ratio ν. These results are also widely cited in textbooks [25, 26, 27]. In later works, approximations for S and I_y for different corrugated shapes were obtained [28, 25, 29, 30]. A review of different approximate formulas of S and I_y for various corrugation shapes can be found in Luo et al. [31]. This is not needed as it is easy to evaluate the two integrals in Eq. (7) accurately for any given corrugated shape using computers nowadays.

Please cite as: http://dx.doi.org/10.1016/j.ijsolstr.2014.02.025

Later Briassoulis [18] proposed the following modified relations

$$
\begin{aligned}
D_{11} &= \frac{\varepsilon}{S}\frac{Eh^3}{12(1-\nu^2)}, \qquad D_{12} = \nu D_{11}, \\
D_{22} &= \frac{EhT^2}{2} + \frac{Eh^3}{12(1-\nu^2)}, \qquad D_{66} = \frac{Eh^3}{24(1+\nu)}.
\end{aligned} \tag{10}
$$

Here T is the rise of the corrugations measured to middle surface as shown in Fig. 3. Briassoulis correctly recognized D_{12} due to the Poisson's effect. However, as will be shown later, the formulas for D_{22} and D_{66} are not correct. The expression for D_{22} is obtained by assuming a sinusoidal corrugated profile, $x_3 = T\sin(2\pi x/\varepsilon)$. Briassoulis's relations are also used in [32, 33, 34] with D_{22} modified in [32] for a trapezoidal corrugated profile.

Very recently, Xia *et al.* [19] obtained the following formulas for bending stiffnesses

$$
\begin{aligned}
D_{11} &= \frac{\varepsilon}{S}\frac{Eh^3}{12(1-\nu^2)}, \qquad D_{12} = \nu D_{11}, \\
D_{22} &= \frac{EI_y}{1-\nu^2} + \left\langle \frac{1}{\sqrt{a}} \right\rangle \frac{Eh^3}{12(1-\nu^2)}, \qquad D_{66} = \frac{S}{\varepsilon}\frac{Eh^3}{24(1+\nu)}.
\end{aligned} \tag{11}
$$

There are other bending stiffnesses proposed in the literature such as those cited by [35] from [36, 37] which are not listed here because they are not as complete and accurate as those listed here.

The equivalent extension stiffnesses were originally found for applications such as roofs and shear walls in 1960-70s [38, 39, 40, 41, 42, 37]. The commonly accepted formulas in literature are:

$$
A_{11} = \frac{Eh^3}{6(1-\nu^2)T^2}, \quad A_{12} = \nu A_{11}, \quad A_{22} = \frac{S}{\varepsilon}Eh, \quad A_{66} = \frac{\varepsilon}{S}\frac{Eh}{2(1+\nu)}. \tag{12}
$$

Later, in [18], Briassoulis provided different formulas for A_{11} and A_{66}

$$
A_{11} = \frac{Eh^3}{h^2 + 6(1-\nu^2)T^2\left(\frac{S^2}{\varepsilon^2} - \frac{S}{2\pi\varepsilon}\sin\frac{2\pi S}{\varepsilon}\right)}, \quad A_{66} = \frac{Eh}{2(1+\nu)}. \tag{13}
$$

with $A_{12} = \nu A_{11}$ and A_{22} the same as that in Eq. (12). Again, the expression for A_{11} is obtained by assuming a sinusoidal corrugated profile, $x_3 = T\sin(2\pi x/\varepsilon)$.

Very recently, Xia *et al.* [19] obtained the following formulas for extension

Please cite as: http://dx.doi.org/10.1016/j.ijsolstr.2014.02.025

stiffnesses

$$\begin{aligned} A_{11} &= \frac{Eh^3}{12(1-\nu^2)} \frac{1}{\left\langle \frac{1}{\sqrt{a}} \right\rangle \frac{h^2}{12} + \frac{I_y}{h}}, \qquad A_{12} = \nu A_{11}, \\ A_{22} &= \nu^2 A_{11} + \frac{S}{\varepsilon} Eh \left(\frac{1}{1-\nu^2} - \frac{1-\nu^2}{4(1+\nu)^2} \right), \qquad A_{66} = \frac{\varepsilon}{S} \frac{Eh}{2(1+\nu)}. \end{aligned} \tag{14}$$

Andrianov et al. [20, 21, 22, 23] obtained different equations by asymptotic analysis of elasticity equations, but the origin of deviations remains unclear.

2.2 Present results

We obtained the following general relations for the equivalent plate stiffnesses for corrugated structures:

$$\begin{aligned} A_{11} &= \frac{E}{1-\nu^2} \frac{12\varepsilon^2 \langle \varphi \mathcal{A} \rangle}{h\mathcal{C}^2} + \frac{Eh}{1-\nu^2} \left\langle \frac{1}{\sqrt{a}} \right\rangle \frac{1}{\mathcal{C}^2}, \quad A_{12} = \nu A_{11}, \\ A_{22} &= Eh \left\langle \sqrt{a} \right\rangle + \nu^2 A_{11}, \quad A_{66} = \mu h \alpha_1, \\ B_{11} &= \frac{E}{1-\nu^2} \frac{12\varepsilon^3 \langle \varphi \mathcal{A} \rangle}{h\mathcal{C}^2} \mathcal{B} + \frac{Eh}{1-\nu^2} \left\langle \frac{1}{\sqrt{a}} \right\rangle \frac{1}{\mathcal{C}^2} \mathcal{B}\varepsilon, \quad B_{12} = \nu B_{11}, \\ B_{22} &= Eh\varepsilon \left\langle \sqrt{a}\phi \right\rangle + \nu^2 B_{11}, \quad B_{66} = \mu h \alpha_2, \\ D_{11} &= \frac{Eh^3}{12(1-\nu^2)} \left(\frac{12^2 \varepsilon^4 \mathcal{B}^2}{h^4 \mathcal{C}^2} \langle \varphi \mathcal{A} \rangle + \frac{1}{\langle \sqrt{a} \rangle} \right) + \frac{Eh}{1-\nu^2} \frac{\varepsilon^2 \mathcal{B}^2}{\mathcal{C}^2} \left\langle \frac{1}{\sqrt{a}} \right\rangle, \\ D_{22} &= Eh\varepsilon^2 \left\langle \phi^2 \sqrt{a} \right\rangle + \frac{Eh^3}{12} \left\langle \frac{1}{\sqrt{a}} \right\rangle + \nu^2 D_{11}, \quad D_{12} = \nu D_{11}, \\ D_{66} &= \frac{\mu h}{4} \left\langle \frac{\sqrt{a}}{3} h^2 - \frac{1}{\sqrt{a}} \frac{\frac{h^4 \varphi'^2}{12^2 \varepsilon^2 a^2} - a\alpha_2^2}{1 + \frac{\varphi'^2 h^2}{48\varepsilon^2 a^3}} \right\rangle. \end{aligned} \tag{15}$$

where

$$\begin{aligned} \mathcal{B} &= \frac{\langle \sqrt{a}\phi \rangle}{\langle \sqrt{a} \rangle}, \qquad \mathcal{C} = -12 \langle \varphi \mathcal{A} \rangle \frac{\varepsilon^2}{h^2} - \left\langle \frac{1}{\sqrt{a}} \right\rangle, \\ \alpha_1 &= 1 \Big/ \left\langle \frac{\sqrt{a}}{1 + \frac{\varphi'^2 h^2}{48\varepsilon^2 a^3}} \right\rangle, \qquad \alpha_2 = \alpha_1 \left\langle \frac{\frac{h^2 \varphi'}{12\varepsilon a}}{1 + \frac{\varphi'^2 h^2}{48\varepsilon^2 a^3}} \right\rangle, \end{aligned} \tag{16}$$

and

$$\mathcal{A}(X) = -\int_0^X \sqrt{a}\phi(Y)dY + \mathcal{B} \int_0^X \sqrt{a}dY \tag{17}$$

We also obtained the following relations for us to recover the shell strains in

Please cite as: http://dx.doi.org/10.1016/j.ijsolstr.2014.02.025

the original corrugated structure:

$$
\begin{aligned}
\gamma_{11}^0 =& c_1\sqrt{a} - \nu a(\epsilon_{yy} + x_3\kappa_{yy}),\\
2\gamma_{12}^0 =& \frac{\sqrt{a}c_2 - \frac{h^2\varphi'\kappa_{xy}}{12\varepsilon a}}{1 + \frac{\varphi'^2 h^2}{48\varepsilon^2 a^3}},\\
\gamma_{22}^0 =& \epsilon_{yy} + x_3\kappa_{yy},\\
\rho_{11}^0 =& a\left(c_1\frac{12x_3}{h^2} + c_4\right) + \nu\sqrt{a}\kappa_{yy},\\
2\rho_{12}^0 =& -\frac{2\sqrt{a}\kappa_{xy} + \frac{\varphi'}{2\varepsilon a}c_2}{1 + \frac{\varphi'^2 h^2}{48\varepsilon^2 a^3}},\\
\rho_{22}^0 =& -\frac{1}{\sqrt{a}}\kappa_{yy}.
\end{aligned}
\tag{18}
$$

with

$$c_1 = \frac{\varepsilon\mathcal{B}(v_{3,11} + \nu v_{3,22}) - (v_{1,1} + \nu v_{2,2})}{\mathcal{C}}, \tag{19}$$

$$c_2 = \alpha_1(v_{1,2} + v_{2,1}) - \alpha_2 v_{3,12}, \tag{20}$$

$$c_4 = \frac{1}{\langle\sqrt{a}\rangle}(v_{3,11} + \nu v_{3,22}) - \frac{12}{h^2}c_1\frac{\langle x_3\sqrt{a}\rangle}{\langle\sqrt{a}\rangle}. \tag{21}$$

In general, the coupling stiffnesses, B_{ij}, are not zero. They vanish, however, for symmetric corrugations of which $\phi(X)$ is an odd function of X.

$$-\phi(X) = \phi(-X), \tag{22}$$

and due to periodicity of $\phi(X)$,

$$\phi(1/2) = 0. \tag{23}$$

Derivative $\varphi = d\phi/dX$ is an even function, and so is $a = 1 + \varphi^2$. Therefore, $\phi\sqrt{a}$ is an odd function and

$$\left\langle\phi\sqrt{a}\right\rangle = 0. \tag{24}$$

Thus $\mathcal{B} = 0$. Derivative φ' is an odd function thus

$$\alpha_2 = 0. \tag{25}$$

The equivalent plate stiffnesses can be simplified for a symmetric corrugation

Please cite as: http://dx.doi.org/10.1016/j.ijsolstr.2014.02.025

as

$$
\begin{aligned}
&A_{11} = \frac{E}{1-\nu^2}\frac{12\varepsilon^2 \langle \varphi \mathcal{A} \rangle}{h\mathcal{C}^2} + \frac{Eh}{1-\nu^2}\left\langle \frac{1}{\sqrt{a}} \right\rangle \frac{1}{\mathcal{C}^2}, \quad A_{12} = \nu A_{11}, \\
&A_{22} = Eh\left\langle \sqrt{a} \right\rangle + \nu^2 A_{11}, \quad A_{66} = \mu h \alpha_1, \\
&B_{11} = B_{12} = B_{22} = B_{66} = 0, \\
&D_{11} = \frac{Eh^3}{12(1-\nu^2)}\frac{1}{\langle \sqrt{a} \rangle}, \\
&D_{22} = Eh\varepsilon^2 \left\langle \phi^2 \sqrt{a} \right\rangle + \frac{Eh^3}{12}\left\langle \frac{1}{\sqrt{a}} \right\rangle + \nu^2 D_{11}, \quad D_{12} = \nu D_{11}, \\
&D_{66} = \frac{\mu h}{4}\left\langle \frac{\sqrt{a}}{3}h^2 - \frac{1}{\sqrt{a}}\frac{\frac{h^4 \varphi'^2}{12^2\varepsilon^2 a^2}}{1+\frac{\varphi'^2 h^2}{48\varepsilon^2 a^3}} \right\rangle .
\end{aligned}
\tag{26}
$$

The formulas for c_1, c_2, c_4 needed for recovery relations in Eq. (18) can also be simplified for a symmetric corrugation.

$$
c_1 = -\frac{(v_{1,1} + \nu v_{2,2})}{\mathcal{C}}, \tag{27}
$$

$$
c_2 = \alpha_1 (v_{1,2} + v_{2,1}), \tag{28}
$$

$$
c_4 = \frac{1}{\langle \sqrt{a} \rangle}(v_{3,11} + \nu v_{3,22}). \tag{29}
$$

2.3 Discussion of the results

First, we perform a simple consistence check for all the results. For equivalent plate stiffnesses to be valid for general corrugated structures, they should be able to reproduce the well-known classical plate stiffnesses when the corrugated structure degenerated to be a flat plate, for which we have

$$
\varphi = \phi = \mathcal{A} = \mathcal{B} = 0, \quad \sqrt{a} = 1, \quad \mathcal{C} = -1, \quad \alpha_1 = 1, \quad \alpha_2 = 0. \tag{30}
$$

The expressions in Eq. (15) can be simplified as

$$
\begin{aligned}
&A_{11} = \frac{Eh}{1-\nu^2}, \quad A_{12} = \nu A_{11}, \quad A_{22} = \frac{Eh}{1-\nu^2}, \quad A_{66} = \frac{Eh}{2(1+\nu)}, \\
&B_{11} = 0, \quad B_{12} = 0, \quad B_{22} = 0, \quad B_{66} = 0, \\
&D_{11} = \frac{Eh^3}{12(1-\nu^2)}, \quad D_{12} = \nu D_{11} \\
&D_{22} = \frac{Eh^3}{12(1-\nu^2)}, \quad D_{66} = \frac{Eh^3}{24(1+\nu)}.
\end{aligned}
\tag{31}
$$

Please cite as: http://dx.doi.org/10.1016/j.ijsolstr.2014.02.025

which are the well known stiffness formulas for the classical model of isotropic homogeneous plates.

The bending stiffnesses in Eq. (9) cannot reproduce the case of a flat plate while those in Eqs. (10) and (11) can. However, none of the extension stiffness from previous studies can reproduce the case of a flat plate.

For shallow corrugation, we know $\phi \sim \delta \ll 1$ and no specific order can be said regarding the magnitude of $\frac{h}{\varepsilon}$. We can use this small parameter to simplify our formulas. We have

$$\mathcal{B} \sim \delta, \quad \mathcal{C} = -\left\langle \frac{1}{\sqrt{a}} \right\rangle, \quad \alpha_1 = \frac{1}{\langle \sqrt{a} \rangle}, \quad \alpha_2 = \alpha_1 \left\langle \frac{h^2 \varphi'}{12 \varepsilon a} \right\rangle \sim \delta. \tag{32}$$

The leading terms of the equivalent plate stiffness are

$$\begin{aligned}
A_{11} &= \frac{Eh}{1-\nu^2} \frac{1}{\left\langle \frac{1}{\sqrt{a}} \right\rangle}, \quad A_{12} = \nu A_{11}, \\
A_{22} &= Eh \left\langle \sqrt{a} \right\rangle + \nu^2 A_{11}, \quad A_{66} = \frac{\mu h}{\langle \sqrt{a} \rangle}, \\
B_{11} &= \frac{Eh}{1-\nu^2} \frac{1}{\left\langle \frac{1}{\sqrt{a}} \right\rangle} \mathcal{B} \varepsilon, \quad B_{12} = \nu B_{11}, \\
B_{22} &= Eh\varepsilon \left\langle \sqrt{a} \phi \right\rangle + \nu^2 B_{11}, \quad B_{66} = \mu h \alpha_2, \\
D_{11} &= \frac{Eh^3}{12(1-\nu^2)} \frac{1}{\langle \sqrt{a} \rangle}, \quad D_{12} = \nu D_{11} \\
D_{22} &= \frac{Eh^3}{12} \left\langle \frac{1}{\sqrt{a}} \right\rangle + \nu^2 D_{11}, \quad D_{66} = \frac{\mu h^2}{12} \left\langle \sqrt{a} \right\rangle.
\end{aligned} \tag{33}$$

Note B_{ij} vanish for symmetric corrugations. The above formulas can degenerate to those for a flat plate. Comparing to the results from previous studies, we can see that Seydel's formulas [24] for D_{11} and D_{66} in Eq. (9) can be used for shallow corrugations. However D_{12} and D_{22} are not valid for shallow corrugations. Briassoulis' formulas [18] for D_{11} and D_{12} in Eq. (10) are valid for shallow corrugations but D_{22} and D_{66} are not valid. The formulas of Xia *et al.* [19] in Eq. (11) can be used for shallow corrugations except D_{22}.

For most corrugated structures, we have $h/\varepsilon \ll 1$. This small parameter can be used to simplify our formulas. We have

$$\mathcal{C} \approx -12 \langle \varphi \mathcal{A} \rangle \frac{\varepsilon^2}{h^2}, \quad \alpha_1 \approx \frac{1}{\langle \sqrt{a} \rangle} \tag{34}$$

Please cite as: http://dx.doi.org/10.1016/j.ijsolstr.2014.02.025

The leading terms of equivalent plate stiffnesses become:

$$\begin{aligned}
&A_{11} = \frac{Eh^3}{12(1-\nu^2)\varepsilon^2 \langle \varphi\mathcal{A} \rangle}, \quad A_{12} = \nu A_{11}, \quad A_{22} = Eh\left\langle \sqrt{a} \right\rangle, \\
&A_{66} = \frac{\mu h}{\langle \sqrt{a} \rangle}, \quad B_{11} = \frac{Eh^3\mathcal{B}}{12(1-\nu^2)\varepsilon \langle \varphi\mathcal{A} \rangle}, \quad B_{12} = \nu B_{11}, \\
&B_{22} = Eh\varepsilon\left\langle \phi\sqrt{a} \right\rangle, \quad B_{66} = \frac{\mu h^3}{12\varepsilon} \frac{\left\langle \frac{\varphi'}{a} \right\rangle}{\langle \sqrt{a} \rangle}, \\
&D_{11} = \frac{Eh^3}{12(1-\nu^2)} \left(\frac{\mathcal{B}^2}{\langle \varphi\mathcal{A} \rangle} + \frac{1}{\langle \sqrt{a} \rangle} \right), \quad D_{12} = \nu D_{11}, \\
&D_{22} = Eh\varepsilon^2\left\langle \phi^2\sqrt{a} \right\rangle, \quad D_{66} = \frac{\mu h^3}{12}\left\langle \sqrt{a} \right\rangle.
\end{aligned} \tag{35}$$

As follows from Eq. (35), among the extension stiffnesses the largest ones are A_{22} and A_{66}, while A_{11} and A_{12} contain small factor $(h/\varepsilon)^2$:

$$A_{11} \sim A_{12} \sim \left(\frac{h}{\varepsilon}\right)^2 A_{22} \sim \left(\frac{h}{\varepsilon}\right)^2 A_{66}. \tag{36}$$

This corresponds to softness of the corrugated plate in the direction of corrugation. Similarly, for bending stiffnesses, the largest stiffness is D_{22}, and

$$D_{11} \sim D_{12} \sim \left(\frac{h}{\varepsilon}\right)^2 D_{22} \sim D_{66}. \tag{37}$$

Among the coupling stiffnesses the largest one is B_{22}, while

$$B_{11} \sim B_{12} \sim \left(\frac{h}{\varepsilon}\right)^2 B_{22} \sim B_{66}. \tag{38}$$

The equivalent plate stiffness for symmetric corrugations have the form:

$$\begin{aligned}
&A_{11} = \frac{Eh^3}{12(1-\nu^2)\varepsilon^2 \langle \phi^2\sqrt{a} \rangle}, \quad A_{12} = \nu A_{11}, \quad A_{22} = Eh\left\langle \sqrt{a} \right\rangle, \\
&A_{66} = \frac{\mu h}{\langle \sqrt{a} \rangle}, \quad D_{11} = \frac{Eh^3}{12(1-\nu^2)\langle \sqrt{a} \rangle}, \quad D_{12} = \nu D_{11}, \\
&D_{22} = Eh\varepsilon^2\left\langle \phi^2\sqrt{a} \right\rangle, \quad D_{66} = \frac{\mu h^3}{12}\left\langle \sqrt{a} \right\rangle.
\end{aligned} \tag{39}$$

Comparing to the results from previous studies, we can see that Seydel [24] obtained the correct bending stiffnesses except D_{12} in Eq. (9), Briassoulis [18] obtained the correct bending stiffnesses except D_{22} and D_{66} in Eq. (10). Xia *et al.* [19] obtained the correct bending stiffnesses except D_{22} in Eq. (11).

Please cite as: http://dx.doi.org/10.1016/j.ijsolstr.2014.02.025

As far as extension stiffnesses are concerned, the commonly accepted formulas in 1960-70s, Eq. (12), are correct if T^2 is defined as half of the average of x_3^2 over the corrugated profile, *i.e.* $T^2 = \frac{\langle x_3^2\sqrt{a}\rangle}{2}$. The modified extension stiffnesses in Eq. (13) by Briassoulis [18] are in fact wrong. The first three formulas of the extension stiffnesses by Xia *et al.* [19] in Eq. (14) are correct if higher order term in A_{11} is neglected. A_{22} is approximately correct as the term $\frac{1}{1-\nu^2} - \frac{1-\nu^2}{4(1+\nu)^2}$ is very close to unity for normal materials.

Most of the previous studies focused on obtained the equivalent plate stiffnesses without paying attention to the local stress/strain field within the original corrugated structure, expect Briassoulis attempted to recover the local stress based on the forces and moments obtained from the equivalent plate analysis in [18]. Such relations are derived based on an assumed sinusoidal corrugated profile. However, as we have already shown that half of the equivalent plate bending and extension stiffnesses from [18] are not correct. The accuracy of the recovery relations can only become worse. Hence, Briassoulis' recovery relations are not listed here and compared with ours.

3 Shell Formulation of Corrugated Structures

The thin-walled corrugated structure can be accurately described by the classical shell theory. Here we summarize the basic equations. We choose a Cartesian coordinate system x_i with basic vectors $\hat{\boldsymbol{e}}_i$. Throughout the paper, Latin indices run through the values 1, 2, and 3; Greek indices assume values 1 and 2, and summation is conducted over repeated indices except where explicitly indicated. The position vector of the shell mid-surface can be considered as a function of coordinates x_1 and x_2:

$$\mathbf{r}(x_1, x_2) = x_1\hat{\boldsymbol{e}}_1 + x_2\hat{\boldsymbol{e}}_2 + x_3\hat{\boldsymbol{e}}_3. \tag{40}$$

If there are corrugations along both x and y directions, x_3 is a function of both coordinates x_1 and x_2. Herein, we restrict our consideration to the case of periodic corrugations in one direction, x, as in Fig. 2. The tangent vectors $\mathbf{a}_\alpha$ of the shell surface can be obtained by differentiating the position vector with respect to x_α, $\mathbf{a}_\alpha = \partial\mathbf{r}/\partial x_\alpha$, so that

$$\mathbf{a}_1 = \hat{\boldsymbol{e}}_1 + \varphi(x)\hat{\boldsymbol{e}}_3, \qquad \mathbf{a}_2 = \hat{\boldsymbol{e}}_2, \tag{41}$$

with

$$\varphi(x) = \frac{dx_3(x)}{dx}. \tag{42}$$

For brevity uses, we also write $\mathbf{a}_\alpha = r_\alpha^i\hat{\boldsymbol{e}}_i$, which implies

$$r_1^1 = 1, \quad r_1^2 = 0, \quad r_1^3 = \varphi(x), \quad r_2^1 = 0, \quad r_2^2 = 1, \quad r_2^3 = 0. \tag{43}$$

Please cite as: http://dx.doi.org/10.1016/j.ijsolstr.2014.02.025

The metric tensor of the shell surface, $a_{\alpha\beta}$, defined as

$$a_{\alpha\beta} = \mathbf{a}_\alpha \cdot \mathbf{a}_\beta, \tag{44}$$

that is

$$a_{11} = 1 + \varphi^2, \qquad a_{12} = 0, \qquad a_{22} = 1, \qquad a = \det \|a_{\alpha\beta}\| = 1 + \varphi^2. \tag{45}$$

The contravariant components of the surface metric tensor $a^{\alpha\beta}$ are the components of the inverse matrix to the matrix $\|a_{\alpha\beta}\|$, i.e. $a^{\alpha\beta}a_{\gamma\beta} = \delta_{\alpha\gamma}$, $\delta_{\alpha\gamma}$ being the two-dimensional Kronecker symbol. We have from Eq. (45)

$$a^{11} = \frac{1}{1+\varphi^2}, \qquad a^{12} = 0, \qquad a^{22} = 1. \tag{46}$$

The normal vector of the shell mid-surface is:

$$\hat{\mathbf{n}} = \frac{\mathbf{a}_1 \times \mathbf{a}_2}{|\mathbf{a}_1 \times \mathbf{a}_2|} = \frac{-\varphi}{\sqrt{a}}\hat{\boldsymbol{e}}_1 + \frac{1}{\sqrt{a}}\hat{\boldsymbol{e}}_3, \tag{47}$$

or in terms of the components,

$$n_1 = -\frac{\varphi}{\sqrt{a}}, \quad n_2 = 0, \quad n_3 = \frac{1}{\sqrt{a}}. \tag{48}$$

The second quadratic form of the shell mid-surface is defined as

$$b_{\alpha\beta} = \frac{\partial \mathbf{a}_\alpha}{\partial x_\beta} \cdot \hat{\mathbf{n}}. \tag{49}$$

Hence, we have

$$\begin{aligned} b_{11} &= \frac{1}{\sqrt{a}}\frac{d\varphi}{dx}, \quad b_{12} = b_{22} = 0, \\ b_1^1 &= \frac{1}{a^{3/2}}\frac{d\varphi}{dx}, \quad b_1^2 = b_2^1 = b_2^2 = 0, \end{aligned} \tag{50}$$

where $b_\beta^\alpha = a^{\alpha\gamma}b_{\gamma\beta}$.

The Christoffel symbols can be found from the equation:

$$\Gamma_{\alpha\beta}^\gamma = \frac{1}{2}a^{\gamma\delta}\left(\frac{\partial a_{\alpha\delta}}{\partial x_\beta} + \frac{\partial a_{\beta\delta}}{\partial x_\alpha} - \frac{\partial a_{\alpha\beta}}{\partial x_\delta}\right). \tag{51}$$

Using Eq. (45), we obtain that all components of $\Gamma_{\alpha\beta}^\gamma$ vanish except

$$\Gamma_{11}^1 = \frac{1}{2a}\frac{da}{dx} = \frac{1}{2}\frac{d\ln a}{dx} \tag{52}$$

Please cite as: http://dx.doi.org/10.1016/j.ijsolstr.2014.02.025

According to the general theory of periodic structures [43, 44] (see also [45] chapter 17), the functions describing the behavior of the shell should be considered as functions of the cell coordinate X, and slow coordinates x, and y. All the geometric characteristics we just introduced are functions of X only, e.g.

$$\begin{aligned} x_3 =& \varepsilon\phi(X), \quad \varphi(X) = \frac{d\phi(X)}{dX}, \\ b_{11} =& \frac{1}{\varepsilon\sqrt{a}}\frac{d\varphi}{dX}, \quad b_1^1 = \frac{1}{\varepsilon a^{3/2}}\frac{d\varphi}{dX}, \quad \Gamma_{11}^1 = \frac{1}{2\varepsilon}\frac{d\ln a}{dX}. \end{aligned} \tag{53}$$

Let $u_i(X,x,y)$ be the components of the displacement vector. The extension strains $\gamma_{\alpha\beta}$ and bending strains $\rho_{\alpha\beta}$ are expressed in terms of u_i as follows [45]:

$$\begin{aligned} 2\gamma_{\alpha\beta} &= r_\alpha^i \frac{\partial u_i}{\partial x_\beta} + r_\beta^i \frac{\partial u_i}{\partial x_\alpha} \\ 2\rho_{\alpha\beta} &= \frac{\partial}{\partial x_\beta}\left(n_i \frac{\partial u^i}{\partial x_\alpha}\right) + \frac{\partial}{\partial x_\alpha}\left(n_i \frac{\partial u^i}{\partial x_\beta}\right) - 2\Gamma_{\alpha\beta}^\gamma n_i \frac{\partial u^i}{\partial x_\gamma} + \theta\left(e_{\gamma\alpha} b_\beta^\gamma + e_{\gamma\beta} b_\alpha^\gamma\right) \end{aligned} \tag{54}$$

where $e_{\alpha\beta}$ denotes surface Levi-Civita tensor ($e_{11} = e_{22} = 0, e_{12} = -e_{21} = \sqrt{a}$). θ is the angle of rotation of the surface elements around the normal vector:

$$\theta = \frac{1}{2\sqrt{a}}\left(r_1^i \frac{\partial u_i}{\partial x_2} - r_2^i \frac{\partial u_i}{\partial x_1}\right) \tag{55}$$

Note that $u^i = u_i$ because u_i are the displacement components in the Cartesian coordinate systems $\hat{\boldsymbol{e}}_i$. While $\gamma_{\alpha\beta}$ and $\rho_{\alpha\beta}$ are tensor components in surface coordinates, and, therefore the components with upper indices acquire additional metric factors. Because X is related with $x = x_1$ according to Eq. (2), the derivative with respect to x_1 can be expressed as

$$\frac{\partial u_i}{\partial x_1} = \frac{\partial u_i}{\partial x} = \frac{\partial u_i}{\partial X}\frac{\partial X}{\partial x}|_{x=\text{const}} + \frac{\partial u_i}{\partial x}|_{X=\text{const}} = \frac{1}{\varepsilon}u_i' + u_{i,1}, \tag{56}$$

with $u_i' = \frac{\partial u_i}{\partial X}|_{x=\text{const}}$ and $u_{i,1} = \frac{\partial u_i}{\partial x}|_{X=\text{const}}$. We also denote $u_{i,2} = \frac{\partial u_i}{\partial x_2} = \frac{\partial u_i}{\partial y}$.

The elastic behavior of the shell is governed by its strain energy density which is given by the following expression:

$$\begin{aligned} \Phi =& \mu h\left(\sigma\left(a^{\alpha\beta}\gamma_{\alpha\beta}\right)^2 + a^{\alpha\beta}a^{\gamma\delta}\gamma_{\alpha\gamma}\gamma_{\beta\delta}\right) \\ &+ \frac{\mu h^3}{12}\left(\sigma\left(a^{\alpha\beta}\rho_{\alpha\beta}\right)^2 + a^{\alpha\beta}a^{\gamma\delta}\rho_{\alpha\gamma}\rho_{\beta\delta}\right). \end{aligned} \tag{57}$$

Here in Eq. (57) $\mu = E/2(1+\nu)$ is the shear modulus, ν the Poisson's ratio, and $\sigma = \nu/(1-\nu)$. The first part is the extension energy and second part the

Please cite as: http://dx.doi.org/10.1016/j.ijsolstr.2014.02.025

bending energy. The strain energy of the unit cell can be written as

$$\begin{aligned} J =& \left\langle \Phi\sqrt{a} \right\rangle \\ =& \left\langle \mu h\sqrt{a} \left(\sigma \left(\frac{1}{a}\gamma_{11} + \gamma_{22} \right)^2 + \frac{1}{a^2}\gamma_{11}^2 + \frac{2}{a}\gamma_{12}^2 + \gamma_{22}^2 \right) \right\rangle \\ &+ \left\langle \frac{\mu h^3}{12}\sqrt{a} \left(\sigma \left(\frac{1}{a}\rho_{11} + \rho_{22} \right)^2 + \frac{1}{a^2}\rho_{11}^2 + \frac{2}{a}\rho_{12}^2 + \rho_{22}^2 \right) \right\rangle \\ =& \left\langle \mu h\sqrt{a} \left((1+\sigma) \left(\frac{\gamma_{11}}{a} + \nu\gamma_{22} \right)^2 + \left(\frac{1+2\sigma}{1+\sigma} \right) \gamma_{22}^2 + \frac{2}{a}\gamma_{12}^2 \right) \right\rangle \\ &+ \left\langle \frac{\mu h^3}{12}\sqrt{a} \left((1+\sigma) \left(\frac{\rho_{11}}{a} + \nu\rho_{22} \right)^2 + \left(\frac{1+2\sigma}{1+\sigma} \right) \rho_{22}^2 + \frac{2}{a}\rho_{12}^2 \right) \right\rangle \end{aligned} \tag{58}$$

with $\nu = \sigma/(1+\sigma)$. Here the material parameters μ, σ and the shell thickness h could be functions of X, but for simplicity, we assume that they are constant.

4 Asymptotic Analysis of the Shell Strain Energy

To model the corrugated structure by an equivalent plate, we start by setting for the shell displacements the presentation following from the general theory of periodic structures [43, 44]:

$$\begin{aligned} u_\alpha(X, x, y) =& v_\alpha(x, y) + \varepsilon\psi_\alpha(X, x, y), \\ u_3(X, x, y) =& v_3(x, y) + \varepsilon\psi_3(X, x, y). \end{aligned} \tag{59}$$

In fact, this is a short cut, and Eq. (59) can be derived by the variational asymptotic method [45], chapter 17.2. In Eq. (59), v_i have the meaning of the effective plate displacements, and ψ_i are some functions which are periodic in X. Without loss of generality, we can define v_i as the average of u_i over the cell:

$$v_i(x, y) = \langle u_i(X, x, y) \rangle \,. \tag{60}$$

Then, obviously,

$$\langle \psi_i(X, x, y) \rangle = 0. \tag{61}$$

Substituting Eq. (59) into Eq. (54) and using Eq. (56), we obtain for the strain

Please cite as: http://dx.doi.org/10.1016/j.ijsolstr.2014.02.025

measures:

$$
\begin{aligned}
\gamma_{11} =& v_{1,1} + \varphi v_{3,1} + \psi_1' + \varphi\psi_3' + \varepsilon\left(\psi_{1,1} + \varphi\psi_{3,1}\right), \\
2\gamma_{12} =& v_{1,2} + v_{2,1} + \varphi v_{3,2} + \psi_2' + \varepsilon\left(\psi_{1,2} + \psi_{2,1} + \varphi\psi_{3,2}\right), \\
\gamma_{22} =& v_{2,2} + \varepsilon\psi_{2,2}, \\
\rho_{11} =& \frac{1}{\varepsilon}U_1' - \frac{1}{2\varepsilon}(\ln a)'U_1 + U_{1,1} = \frac{\sqrt{a}}{\varepsilon}\left(\frac{U_1}{\sqrt{a}}\right)' + U_{1,1}, \\
2\rho_{12} =& U_{1,2} + U_{2,1} + \frac{1}{\varepsilon}U_2' + \frac{\varphi'}{\varepsilon a^{3/2}}\sqrt{a}\theta, \\
\rho_{22} =& U_{2,2}.
\end{aligned} \tag{62}
$$

Here comma in indices denotes derivatives with respect to x_α, prime the derivative with respect to X. Besides, we introduced the notations,

$$U_1 = n_1(v_{1,1} + \psi_1') + n_3(\psi_3' + v_{3,1}) + \varepsilon(n_1\psi_{1,1} + n_3\psi_{3,1}), \tag{63}$$

$$U_2 = n_1 v_{1,2} + n_3 v_{3,2} + \varepsilon(n_1\psi_{1,2} + n_3\psi_{3,2}). \tag{64}$$

Rotation θ can be found from Eq. (55),

$$2\sqrt{a}\theta = v_{1,2} - v_{2,1} + \varphi v_{3,2} - \psi_2' + \varepsilon(\psi_{1,2} - \psi_{2,1} + \varphi\psi_{3,2}).$$

Our objective is to construct an equivalent plate model, i.e. the equations for v_i. To this end, assuming that v_i are known, we seek for the expression of ψ_i in terms of v_i and their derivatives.

4.1 Step 1: discarding doubtful terms

Following the variational asymptotic method, we drop all the terms that are asymptotically small in terms of known small parameters in the energy functional. To model the corrugated structure as a flat plate, we implicitly assume that the corrugated plate is formed by many cells, we have $\varepsilon/L \ll 1$, where L is the characteristic length of macroscopic deformations. Due to the smallness of ε/L, we can drop in the energy the terms associated with derivatives $\psi_{1,1} + \varphi\psi_{3,1}$ in γ_{11}, terms associated with $\psi_{2,1}$ in $2\gamma_{12}$, terms associated with $U_{1,1}$ in ρ_{11}, terms associated with $U_{2,1}$ in $2\rho_{12}$, terms associated with $n_1\psi_{1,1}+n_3\psi_{3,1}$ in U_1, terms associated with $\psi_{2,1}$ in $2\sqrt{a}\theta$, and $U_{2,2}$ in ρ_{22}. However, the terms containing $(\psi_1'+\varphi\psi_3')\psi_{2,2}$, $\psi_2'\left(\psi_{1,2} + \varphi\psi_{3,2}\right)$, $(n_1\psi_{1,2}'+n_3\psi_{3,2}')\psi_2'$ and $(n_1\psi_{1,2} + n_3\psi_{3,2})'\psi_2'$ are doubtful as we do not know the relative orders of ψ_i and there is no clear larger terms than these terms. As suggested in [45], we will first discard them and later to check whether they are indeed asymptotically smaller that the terms we keep. The leading terms of the energy in

Please cite as: http://dx.doi.org/10.1016/j.ijsolstr.2014.02.025

the first approximation are

$$J_0 = \left\langle \mu h\sqrt{a}\left((1+\sigma)\left(\frac{\gamma_{11}^0}{a}+\nu\gamma_{22}^0\right)^2+\left(\frac{1+2\sigma}{1+\sigma}\right)\left(\gamma_{22}^0\right)^2+\frac{2}{a}\left(\gamma_{12}^0\right)^2\right)\right\rangle + \left\langle \frac{\mu h^3}{12}\sqrt{a}\left((1+\sigma)\left(\frac{\rho_{11}^0}{a}+\nu\rho_{22}^0\right)^2+\left(\frac{1+2\sigma}{1+\sigma}\right)\left(\rho_{22}^0\right)^2+\frac{2}{a}\left(\rho_{12}^0\right)^2\right)\right\rangle \tag{65}$$

with

$$\begin{aligned} \gamma_{11}^0 =& v_{1,1}+\varphi v_{3,1}+\psi_1'+\varphi\psi_3', \\ 2\gamma_{12}^0 =& v_{1,2}+v_{2,1}+\varphi v_{3,2}+\psi_2', \\ \gamma_{22}^0 =& v_{2,2}, \\ \rho_{11}^0 =& \frac{\sqrt{a}}{\varepsilon}\left(\frac{U_1^0}{\sqrt{a}}\right)', \\ 2\rho_{12}^0 =& \frac{1}{\varepsilon}U_2^{0\prime}+\frac{\varphi'}{\varepsilon a^{3/2}}\sqrt{a}\theta^0, \\ \rho_{22}^0 =& 0. \end{aligned} \tag{66}$$

and

$$\begin{aligned} U_1^0 &= n_1(v_{1,1}+\psi_1')+n_3(\psi_3'+v_{3,1}) \\ U_2^0 &= n_1 v_{1,2}+n_3 v_{3,2} \\ 2\sqrt{a}\theta^0 &= v_{1,2}-v_{2,1}+\varphi v_{3,2}-\psi_2' \end{aligned} \tag{67}$$

Substituting Eq. (67) into the bending strains in Eq. (66) and considering

$$n_3 - n_1\varphi = \sqrt{a} \qquad n_1' = \frac{-\varphi'}{a^{3/2}} \qquad n_3' = \frac{-\varphi\varphi'}{a^{3/2}}. \tag{68}$$

we have

$$\rho_{11}^0 = \frac{\sqrt{a}}{\varepsilon}\left(\psi_3' - \frac{\varphi}{a}\gamma_{11}^0\right)' \qquad 2\rho_{12}^0 = -\frac{\varphi'}{2\varepsilon a^{3/2}}(2\gamma_{12}^0) \tag{69}$$

$\gamma_{22}^0, \rho_{22}^0$ do not involve ψ_i, $2\gamma_{12}^0, 2\rho_{12}^0$ involve ψ_2 only, and $\gamma_{11}^0, \rho_{11}^0$ involve ψ_1, ψ_3.

Let us focus on solving ψ_2 first. The strain energy in Eq. (65) related with ψ_2 is:

$$J_2 = \left\langle \mu h\frac{1}{2\sqrt{a}}\left(\left(2\gamma_{12}^0\right)^2+\frac{h^2}{12}\left(2\rho_{12}^0\right)^2\right)\right\rangle. \tag{70}$$

We need to minimize $2\gamma_{12}^0, 2\rho_{12}^0$ in Eq. (70) over periodic functions $\psi_2(X)$ subject to the constraints Eq. (61). The constraints can be taken care of by introducing the Lagrange multipliers. The corresponding Euler-Lagrange equation is:

$$\left(\frac{1}{\sqrt{a}}\left(2\gamma_{12}^0 - \frac{h^2}{12}2\rho_{12}^0\frac{\varphi'}{2\varepsilon a^{3/2}}\right)\right)' - \lambda_2 = 0. \tag{71}$$

Please cite as: http://dx.doi.org/10.1016/j.ijsolstr.2014.02.025

along with boundary conditions

$$[\psi_2] = 0, \qquad \left[\frac{1}{\sqrt{a}}\left(2\gamma_{12}^0 - \frac{h^2}{12}2\rho_{12}^0\frac{\varphi'}{2\varepsilon a^{3/2}}\right)\right] = 0. \tag{72}$$

with the square brackets denoting the difference between the end values, for example $[\psi_2] = \psi_2(\frac{1}{2}) - \psi_2(-\frac{1}{2})$. The second condition in Eq. (72) leads to $\lambda_2 = 0$. Hence:

$$\frac{1}{\sqrt{a}}\left(2\gamma_{12}^0 - \frac{h^2}{12}2\rho_{12}^0\frac{\varphi'}{2\varepsilon a^{3/2}}\right) = c_2. \tag{73}$$

Thus:

$$2\gamma_{12}^0 = \frac{\sqrt{a}c_2}{1 + \frac{\varphi'^2 h^2}{48\varepsilon^2 a^3}}, \tag{74}$$

$$v_{1,2} + v_{2,1} + \varphi v_{3,2} + \psi_2' = \frac{\sqrt{a}c_2}{1 + \frac{\varphi'^2 h^2}{48\varepsilon^2 a^3}}. \tag{75}$$

Integrating Eq. (75) over the cell length, we obtain the constant c_2:

$$v_{1,2} + v_{2,1} = \left\langle \frac{\sqrt{a}}{1 + \frac{\varphi'^2 h^2}{48\varepsilon^2 a^3}} \right\rangle c_2, \tag{76}$$

$$c_2 = \alpha_1(v_{1,2} + v_{2,1}). \tag{77}$$

Integrating Eq. (75) with respect to X both sides, we have

$$\psi_2 = -X(v_{1,2} + v_{2,1}) - \phi v_{3,2} + \int_0^X \frac{\sqrt{a}c_2}{1 + \frac{\varphi'^2 h^2}{48\varepsilon^2 a^3}} dY + const. \tag{78}$$

Considering the constraint in Eq. (61), we can integrate both sides of Eq. (78) over the cell length to solve for the constant, and the final expression for ψ_2 is

$$\psi_2 = -X(v_{1,2} + v_{2,1}) - \phi v_{3,2} + \int_0^X \frac{\sqrt{a}c_2}{1 + \frac{\varphi'^2 h^2}{48\varepsilon^2 a^3}} dY - \left\langle \int_0^X \frac{\sqrt{a}c_2}{1 + \frac{\varphi'^2 h^2}{48\varepsilon^2 a^3}} dY \right\rangle. \tag{79}$$

The strain energy in Eq. (65) related with ψ_1 and ψ_3 is:

$$J_1 = \left\langle \mu h\sqrt{a}\,(1+\sigma)\left(\frac{\gamma_{11}^0}{a} + \nu\gamma_{22}^0\right)^2 + \frac{\mu h^3}{12}\sqrt{a}\,(1+\sigma)\left(\frac{\rho_{11}^0}{a} + \nu\rho_{22}^0\right)^2 \right\rangle. \tag{80}$$

Similarly, we use Lagrange multiplier to take care of the constraints of ψ_1 and ψ_3 in Eq. (61). The corresponding Euler-Lagrange equations are:

$$\begin{aligned} &\left(\frac{1}{\sqrt{a}}\left(\frac{\gamma_{11}^0}{a} + \nu\gamma_{22}^0\right) + \frac{h^2}{12\varepsilon}\left(\frac{\rho_{11}^0}{a} + \nu\rho_{22}^0\right)'\frac{\varphi}{a}\right)' - \lambda_1 = 0, \\ &\left(\frac{\varphi}{\sqrt{a}}\left(\frac{\gamma_{11}^0}{a} + \nu\gamma_{22}^0\right) - \frac{h^2}{12\varepsilon}\left(\frac{\rho_{11}^0}{a} + \nu\rho_{22}^0\right)'\frac{1}{a}\right)' - \lambda_3 = 0. \end{aligned} \tag{81}$$

Please cite as: http://dx.doi.org/10.1016/j.ijsolstr.2014.02.025

along with boundary conditions

$$[\psi_1]=0,\qquad [\psi_1']=0,\qquad \left[\frac{1}{\sqrt{a}}\left(\frac{\gamma_{11}^0}{a}+\nu\gamma_{22}^0\right)+\frac{h^2}{12\varepsilon}\left(\frac{\rho_{11}^0}{a}+\nu\rho_{22}^0\right)'\frac{\varphi}{a}\right]=0,$$
$$[\psi_3]=0,\qquad [\psi_3']=0,\qquad \left[\frac{\varphi}{\sqrt{a}}\left(\frac{\gamma_{11}^0}{a}+\nu\gamma_{22}^0\right)-\frac{h^2}{12\varepsilon}\left(\frac{\rho_{11}^0}{a}+\nu\rho_{22}^0\right)'\frac{1}{a}\right]=0,$$
$$\left[\frac{\rho_{11}^0}{a}+\nu\rho_{22}^0\right]=0. \tag{82}$$

The third and sixth conditions in Eq. (82) leads to $\lambda_1=\lambda_3=0$. Hence:

$$\frac{1}{\sqrt{a}}\left(\frac{\gamma_{11}^0}{a}+\nu\gamma_{22}^0\right)+\frac{h^2}{12\varepsilon}\left(\frac{\rho_{11}^0}{a}+\nu\rho_{22}^0\right)'\frac{\varphi}{a}=c_1, \tag{83}$$
$$\frac{\varphi}{\sqrt{a}}\left(\frac{\gamma_{11}^0}{a}+\nu\gamma_{22}^0\right)-\frac{h^2}{12\varepsilon}\left(\frac{\rho_{11}^0}{a}+\nu\rho_{22}^0\right)'\frac{1}{a}=c_3. \tag{84}$$

Integrate ($\varphi\times(83)-(84)$) over the cell length with considering the seventh conditions in Eq. (82) conclude:

$$c_3=0. \tag{85}$$

Then Eqs. (83) and (84) can be simplified as:

$$\left(\frac{\rho_{11}^0}{a}+\nu\rho_{22}^0\right)'=c_1\frac{12\varphi\varepsilon}{h^2}, \tag{86}$$
$$\left(\frac{\gamma_{11}^0}{a}+\nu\gamma_{22}^0\right)=\frac{c_1}{\sqrt{a}}. \tag{87}$$

Integrate Eq. (86)

$$\left(\frac{\rho_{11}^0}{a}+\nu\rho_{22}^0\right)=c_1\frac{12x_3}{h^2}+c_4, \tag{88}$$

Rewrite Eq. (88) considering Eq. (69)

$$\left(\psi_3'-\frac{\varphi}{a}\gamma_{11}^0\right)'=\varepsilon\left(c_1\frac{12}{h^2}x_3\sqrt{a}+c_4\sqrt{a}\right). \tag{89}$$

Integrate over the cell length with the fact $\left[\psi_3'-\frac{\varphi}{a}\gamma_{11}^0\right]=0$, c_4 is:

$$c_4=-\frac{12}{h^2}c_1\frac{\langle x_3\sqrt{a}\rangle}{\langle\sqrt{a}\rangle}. \tag{90}$$

Integrate Eq. (89) considering c_4,

$$\psi_3'-\frac{\varphi}{a}\gamma_{11}^0=-\frac{12\varepsilon^2}{h^2}c_1\mathcal{A}+c_5. \tag{91}$$

Please cite as: http://dx.doi.org/10.1016/j.ijsolstr.2014.02.025

$\varphi \times (87) + (91)$ gives

$$\psi_3' + \nu\varphi\gamma_{22}^0 = \frac{c_1\varphi}{\sqrt{a}} - \frac{12\varepsilon^2}{h^2}c_1\mathcal{A} + c_5, \tag{92}$$

Integrating over the cell length, we obtain

$$c_5 = -c_1\left\langle \frac{\varphi}{\sqrt{a}} \right\rangle + \frac{12\varepsilon^2}{h^2}c_1\left\langle \mathcal{A} \right\rangle. \tag{93}$$

Substitute c_5 into Eq. (92):

$$\psi_3' = -\nu\varphi\gamma_{22}^0 + c_1\left(\frac{\varphi}{\sqrt{a}} - \left\langle \frac{\varphi}{\sqrt{a}} \right\rangle\right) - \frac{12\varepsilon^2}{h^2}c_1(\mathcal{A} - \langle \mathcal{A} \rangle). \tag{94}$$

Rewrite Eq. (87) as

$$v_{1,1} + \varphi v_{3,1} + \psi_1' + \varphi\psi_3' = c_1\sqrt{a} - \nu a\gamma_{22}^0, \tag{95}$$

Substituting Eq. (94) into Eq. (95), we have

$$\psi_1' = -(v_{1,1}+\nu v_{2,2}+\varphi v_{3,1})+c_1\left(\frac{1}{\sqrt{a}} + \varphi\left\langle \frac{\varphi}{\sqrt{a}} \right\rangle\right)+\frac{12\varepsilon^2}{h^2}c_1\left(\varphi\mathcal{A} - \varphi\left\langle \mathcal{A} \right\rangle\right) \tag{96}$$

Integrate over the cell length:

$$v_{1,1} + \nu v_{2,2} = \frac{12\varepsilon^2}{h^2}c_1\left\langle \varphi\mathcal{A} \right\rangle + c_1\left\langle \frac{1}{\sqrt{a}} \right\rangle, \tag{97}$$

which can be used to solve for c_1 as

$$c_1 = -\frac{(v_{1,1} + \nu v_{2,2})}{\mathcal{C}}. \tag{98}$$

Integrating Eq. (94) both sides with respect to X, we have

$$\begin{aligned} \psi_3 = &-\nu\phi\gamma_{22}^0 + c_1\left(\int_0^X \frac{\varphi}{\sqrt{a}}dY - X\left\langle \frac{\varphi}{\sqrt{a}} \right\rangle\right) \\ &- \frac{12\varepsilon^2}{h^2}c_1\left(\int_0^X \mathcal{A}dY - X\left\langle \mathcal{A} \right\rangle\right) + const. \end{aligned} \tag{99}$$

Considering the constraint in Eq. (61), we can integrate both sides of Eq. (99) over the cell length to solve for the constant, and the final expression for ψ_3 is

$$\begin{aligned} \psi_3 = &-\nu\phi\gamma_{22}^0 + c_1\left(\int_0^X \frac{\varphi}{\sqrt{a}}dY - \left\langle \int_0^X \frac{\varphi}{\sqrt{a}}dY \right\rangle - X\left\langle \frac{\varphi}{\sqrt{a}} \right\rangle\right) \\ &- \frac{12\varepsilon^2}{h^2}c_1\left(\int_0^X \mathcal{A}dY - \left\langle \int_0^X \mathcal{A}dY \right\rangle - X\left\langle \mathcal{A} \right\rangle\right). \end{aligned} \tag{100}$$

Please cite as: http://dx.doi.org/10.1016/j.ijsolstr.2014.02.025

Integrating Eq. (96) both sides with respect to X, we have

$$\begin{aligned}\psi_1 =& -\left(Xv_{1,1} + \nu Xv_{2,2} + \phi v_{3,1}\right) + c_1\left(\int_0^X \frac{1}{\sqrt{a}}dY + \phi\left\langle\frac{\varphi}{\sqrt{a}}\right\rangle\right) \\ &+ \frac{12\varepsilon^2}{h^2}c_1\left(\int_0^X \varphi\mathcal{A}dY - \phi\left\langle\mathcal{A}\right\rangle\right) + const\end{aligned} \tag{101}$$

Considering the constraint in Eq. (61), we can integrate both sides of Eq. (101) over the cell length to solve for the constant, and the final expression for ψ_1 is

$$\begin{aligned}\psi_1 =& -\left(Xv_{1,1} + \nu Xv_{2,2} + \phi v_{3,1}\right) \\ &+ c_1\left(\int_0^X \frac{1}{\sqrt{a}}dY - \left\langle\int_0^X \frac{1}{\sqrt{a}}dY\right\rangle + \phi\left\langle\frac{\varphi}{\sqrt{a}}\right\rangle\right) \\ &+ \frac{12\varepsilon^2}{h^2}c_1\left(\int_0^X \varphi\mathcal{A}dY - \left\langle\int_0^X \varphi\mathcal{A}dY\right\rangle - \phi\left\langle\mathcal{A}\right\rangle\right)\end{aligned} \tag{102}$$

4.2 Step 2: corrected with doubtful terms

Inspecting Eqs. (79) and (102), we find out that there are $\phi v_{3,\alpha}$ contained in these two functions. This means we cannot drop the aforementioned terms, $(\psi_1' + \varphi\psi_3')\psi_{2,2}$, $\psi_2'\left(\psi_{1,2} + \varphi\psi_{3,2}\right)$, $(n_1\psi_{1,2}' + n_3\psi_{3,2}')\psi_2'$, and $(n_1\psi_{1,2} + n_3\psi_{3,2})'\psi_2'$ completely, but should keep the major contributions contained in these terms. In the same way, we also need to recover those terms which are of similar orders into the strain expressions. Thus, for γ_{11}^0, we recover $-x_3v_{3,11}$ from the neglected term $\varepsilon\psi_{1,1}$

$$\gamma_{11}^0 = v_{1,1} - x_3v_{3,11} + \varphi v_{3,1} + \psi_1' + \varphi\psi_3' \tag{103}$$

For $2\gamma_{12}^0$, we recover $-2x_3v_{3,12}$ from the neglected terms $\varepsilon(\psi_{1,2} + \psi_{2,1})$

$$2\gamma_{12}^0 = v_{1,2} + v_{2,1} - 2x_3v_{3,12} + \varphi v_{3,2} + \psi_2' \tag{104}$$

For γ_{22}^0, we recover $-x_3v_{3,22}$ from the neglected terms $\varepsilon\psi_{2,2}$

$$\gamma_{22}^0 = v_{2,2} - x_3v_{3,22} \tag{105}$$

For ρ_{11}^0, we recover $(n_3 - n_1\varphi)v_{3,11} = \sqrt{a}v_{3,11}$ from the neglected term $U_{1,1}$

$$\rho_{11}^0 = \frac{\sqrt{a}}{\varepsilon}\left(\frac{U_1^0}{\sqrt{a}}\right)' + \sqrt{a}v_{3,11} \tag{106}$$

For $2\rho_{12}^0$, we recover $(\sqrt{a} + n_3)v_{3,12}$ from the neglected terms in $U_{1,2} + U_{2,1}$

$$2\rho_{12}^0 = (\sqrt{a} + n_3)v_{3,12} + \frac{1}{\varepsilon}U_2^{0\prime} + \frac{\varphi'}{\varepsilon a^{3/2}}\sqrt{a}\theta^0 \tag{107}$$

Please cite as: http://dx.doi.org/10.1016/j.ijsolstr.2014.02.025

For ρ^0_{22}, we recover $n_3v_{3,12}$ from the neglected terms in $U_{2,2}$

$$\rho^0_{22} = n_3v_{3,22} \tag{108}$$

For U^0_1, we recover $-x_3v_{3,11}$ from the neglected term $\varepsilon\psi_{1,1}$

$$U^0_1 = n_1(v_{1,1} - x_3v_{3,11} + \psi'_1) + n_3(\psi'_3 + v_{3,1}) \tag{109}$$

For U^0_2, we recover $-x_3v_{3,12}$ from the neglected term $\varepsilon\psi_{1,2}$

$$U^0_2 = n_1(v_{1,2} - x_3v_{3,12}) + n_3v_{3,2} \tag{110}$$

For θ^0, the major terms contributed from the neglected term $\varepsilon(\psi_{1,2} - \psi_{2,1})$ cancel each other, so that

$$2\sqrt{a}\theta^0 = v_{1,2} - v_{2,1} + \varphi v_{3,2} - \psi'_2 \tag{111}$$

Using Eqs. (109), (110), and (111), we can rewrite the bending strains as

$$\begin{aligned}\rho^0_{11} =& \frac{\sqrt{a}}{\varepsilon}\left(\psi'_3 - \frac{\varphi}{a}\gamma^0_{11}\right)' + \sqrt{a}v_{3,11},\\ 2\rho^0_{12} =& 2\sqrt{a}v_{3,12} - \frac{\varphi'}{2\varepsilon a^{3/2}}(2\gamma^0_{12}),\\ \rho^0_{22} =& \frac{1}{\sqrt{a}}v_{3,22}.\end{aligned} \tag{112}$$

Substituting this new set of strain measures into Eq. (65), we need to carry out the solution procedure again. Most of the equations starting Eq. (70) to Eq. (102) remain the same, except the following changes.

Eq. (74) is replaced with

$$2\gamma^0_{12} = \frac{\sqrt{a}c_2 + \frac{h^2\varphi' v_{3,12}}{12\varepsilon a}}{1 + \frac{\varphi'^2h^2}{48\varepsilon^2a^3}}. \tag{113}$$

Eq. (75) is replaced with

$$v_{1,2} + v_{2,1} - 2x_3v_{3,12} + \varphi v_{3,2} + \psi'_2 = \frac{\sqrt{a}c_2 + \frac{h^2\varphi' v_{3,12}}{12\varepsilon a}}{1 + \frac{\varphi'^2h^2}{48\varepsilon^2a^3}}. \tag{114}$$

Eq. (76) is replaced with

$$v_{1,2} + v_{2,1} = \left\langle \frac{\sqrt{a}}{1 + \frac{\varphi'^2h^2}{48\varepsilon^2a^3}} \right\rangle c_2 + \left\langle \frac{\frac{h^2\varphi'}{12\varepsilon a}}{1 + \frac{\varphi'^2h^2}{48\varepsilon^2a^3}} \right\rangle v_{3,12}, \tag{115}$$

Please cite as: http://dx.doi.org/10.1016/j.ijsolstr.2014.02.025

with c_2 defined in Eq. (20).

Eq. (78) should be replaced with

$$\psi_2 = -X(v_{1,2}+v_{2,1}) - \phi v_{3,2} + 2\int_0^X x_3 dY v_{3,12} + \int_0^X \frac{\sqrt{a}c_2 + \frac{h^2\varphi' v_{3,12}}{12\varepsilon a}}{1+\frac{\varphi'^2 h^2}{48\varepsilon^2 a^3}} dY + const. \tag{116}$$

Eq. (79) should be replaced with

$$\begin{aligned}\psi_2 = &- X(v_{1,2}+v_{2,1}) - \phi v_{3,2} + 2\left(\int_0^X x_3 dY - \left\langle \int_0^X x_3 dY \right\rangle\right) v_{3,12} \\ &+ \int_0^X \frac{\sqrt{a}c_2 + \frac{h^2\varphi' v_{3,12}}{12\varepsilon a}}{1+\frac{\varphi'^2 h^2}{48\varepsilon^2 a^3}} dY - \left\langle \int_0^X \frac{\sqrt{a}c_2 + \frac{h^2\varphi' v_{3,12}}{12\varepsilon a}}{1+\frac{\varphi'^2 h^2}{48\varepsilon^2 a^3}} dY \right\rangle .\end{aligned} \tag{117}$$

Eq. (89) should be replaced with

$$\left(\psi_3' - \frac{\varphi}{a}\gamma_{11}^0\right)' = \varepsilon\left(c_1 \frac{12}{h^2} x_3\sqrt{a} + c_4\sqrt{a} - (v_{3,11} + \nu v_{3,22})\right). \tag{118}$$

with c_4 defined in Eq. (21).

Eq. (91) should be replaced with

$$\psi_3' - \frac{\varphi}{a}\gamma_{11}^0 = -\frac{12\varepsilon^2}{h^2}c_1\mathcal{A} + \varepsilon\left(\frac{\int_0^X \sqrt{a}dY}{\langle\sqrt{a}\rangle} - X\right)(v_{3,11} + \nu v_{3,22}) + c_5. \tag{119}$$

Eq. (92) should be replaced with

$$\psi_3' + \nu\varphi\gamma_{22}^0 = \frac{c_1\varphi}{\sqrt{a}} - \frac{12\varepsilon^2}{h^2}c_1\mathcal{A} + \varepsilon\left(\frac{\int_0^X \sqrt{a}dY}{\langle\sqrt{a}\rangle} - X\right)(v_{3,11} + \nu v_{3,22}) + c_5. \tag{120}$$

Eq. (93) should be replaced with

$$c_5 = -c_1\left\langle\frac{\varphi}{\sqrt{a}}\right\rangle + \frac{12\varepsilon^2}{h^2}c_1\langle\mathcal{A}\rangle - \varepsilon\frac{\left\langle\int_0^X \sqrt{a}dY\right\rangle}{\langle\sqrt{a}\rangle}(v_{3,11} + \nu v_{3,22}). \tag{121}$$

Here, notice $\langle\varphi x_3\rangle = 0$.

Please cite as: http://dx.doi.org/10.1016/j.ijsolstr.2014.02.025

Eq. (94) should be replaced with

$$\begin{aligned}\psi_3' = &-\nu\varphi\gamma_{22}^0 + c_1\left(\frac{\varphi}{\sqrt{a}} - \left\langle\frac{\varphi}{\sqrt{a}}\right\rangle\right) - \frac{12\varepsilon^2}{h^2}c_1(\mathcal{A} - \langle\mathcal{A}\rangle)\\ &+\varepsilon\left(\frac{\int_0^X \sqrt{a}dY - \left\langle\int_0^X \sqrt{a}dY\right\rangle}{\langle\sqrt{a}\rangle} - X\right)(v_{3,11} + \nu v_{3,22}).\end{aligned} \tag{122}$$

Eq. (95) should be replaced with

$$v_{1,1} - x_3 v_{3,11} + \varphi v_{3,1} + \psi_1' + \varphi\psi_3' = c_1\sqrt{a} - \nu a\gamma_{22}^0. \tag{123}$$

Eq. (96) should be replaced with

$$\begin{aligned}\psi_1' = &-(v_{1,1} + \nu v_{2,2} + \varphi v_{3,1}) + x_3(v_{3,11} + \nu v_{3,22})\\ &+ c_1\left(\frac{1}{\sqrt{a}} + \varphi\left\langle\frac{\varphi}{\sqrt{a}}\right\rangle\right) + \frac{12\varepsilon^2}{h^2}c_1\left(\varphi\mathcal{A} - \varphi\left\langle\mathcal{A}\right\rangle\right)\\ &-\varepsilon\left(\frac{\varphi\int_0^X \sqrt{a}dY - \varphi\left\langle\int_0^X \sqrt{a}dY\right\rangle}{\langle\sqrt{a}\rangle} - \varphi X\right)(v_{3,11} + \nu v_{3,22}).\end{aligned} \tag{124}$$

Eq. (97) should be replaced with

$$v_{1,1} + \nu v_{2,2} = \frac{12\varepsilon^2}{h^2}c_1\left\langle\varphi\mathcal{A}\right\rangle + \varepsilon\mathcal{B}(v_{3,11} + \nu v_{3,22}) + c_1\left\langle\frac{1}{\sqrt{a}}\right\rangle. \tag{125}$$

with the constant $\mathcal{B}$

$$\begin{aligned}\mathcal{B} &= \left(\langle\varphi X\rangle - \frac{\left\langle\varphi\int_0^X \sqrt{a}dY\right\rangle}{\langle\sqrt{a}\rangle}\right) = \frac{\langle\sqrt{a}\rangle\int_{-\frac{1}{2}}^{\frac{1}{2}} X d\phi - \int_{-\frac{1}{2}}^{\frac{1}{2}}\int_0^X \sqrt{a}dY d\phi}{\langle\sqrt{a}\rangle}\\ &= \frac{\langle\sqrt{a}\rangle\left(X\phi|_{-\frac{1}{2}}^{\frac{1}{2}} - \langle\phi\rangle\right) - \int_0^X \sqrt{a}dY\,\phi|_{-\frac{1}{2}}^{\frac{1}{2}} + \langle\sqrt{a}\phi\rangle}{\langle\sqrt{a}\rangle} = \frac{\langle\sqrt{a}\phi\rangle}{\langle\sqrt{a}\rangle}.\end{aligned} \tag{126}$$

Eq. (98) should be replaced with the definition in Eq. (19).

Please cite as: http://dx.doi.org/10.1016/j.ijsolstr.2014.02.025

Eq. (99) should be replaced with

$$\begin{aligned}\psi_3 =& -\nu\phi v_{2,2} + \nu\int_0^X \varphi x_3 dY v_{3,22} + c_1\left(\int_0^X \frac{\varphi}{\sqrt{a}}dY - X\left\langle\frac{\varphi}{\sqrt{a}}\right\rangle\right)\\ & - \frac{12\varepsilon^2}{h^2}c_1\left(\int_0^X \mathcal{A}dY - X\left\langle\mathcal{A}\right\rangle\right) + const \\ & + \varepsilon\left(\frac{\int_0^X\int_0^Y\sqrt{a}dZdY - X\left\langle\int_0^X\sqrt{a}dY\right\rangle}{\langle\sqrt{a}\rangle} - \frac{X^2}{2}\right)(v_{3,11} + \nu v_{3,22}).\end{aligned} \tag{127}$$

Eq. (100) should be replaced with

$$\begin{aligned}\psi_3 =& -\nu\phi v_{2,2} + \nu\left(\int_0^X \varphi x_3 dY - \left\langle\int_0^X \varphi x_3 dY\right\rangle\right)v_{3,22}\\ & + c_1\left(\int_0^X \frac{\varphi}{\sqrt{a}}dY - \left\langle\int_0^X \frac{\varphi}{\sqrt{a}}dY\right\rangle - X\left\langle\frac{\varphi}{\sqrt{a}}\right\rangle\right)\\ & - \frac{12\varepsilon^2}{h^2}c_1\left(\int_0^X \mathcal{A}dY - \left\langle\int_0^X \mathcal{A}dY\right\rangle - X\left\langle\mathcal{A}\right\rangle\right)\\ & + \varepsilon\left(\frac{\int_0^X\int_0^Y\sqrt{a}dZdY - \left\langle\int_0^X\int_0^Y\sqrt{a}dZdY\right\rangle - X\left\langle\int_0^X\sqrt{a}dY\right\rangle}{\langle\sqrt{a}\rangle} - \frac{X^2}{2} + \frac{1}{24}\right)(v_{3,11} + \nu v_{3,22}).\end{aligned} \tag{128}$$

Eq. (101) should be replaced with

$$\begin{aligned}\psi_1 =& -(Xv_{1,1} + \nu X v_{2,2} + \phi v_{3,1}) + \int_0^X x_3 dY(v_{3,11} + \nu v_{3,22})\\ & + c_1\left(\int_0^X \frac{1}{\sqrt{a}}dY + \phi\left\langle\frac{\varphi}{\sqrt{a}}\right\rangle\right) + \frac{12\varepsilon^2}{h^2}c_1\left(\int_0^X \varphi\mathcal{A}dY - \phi\left\langle\mathcal{A}\right\rangle\right) + const\\ & - \varepsilon\left(\frac{\int_0^X\varphi\int_0^Y\sqrt{a}dZdY - \phi\left\langle\int_0^X\sqrt{a}dY\right\rangle}{\langle\sqrt{a}\rangle} - \int_0^X \varphi X dY\right)(v_{3,11} + \nu v_{3,22}).\end{aligned} \tag{129}$$

Please cite as: http://dx.doi.org/10.1016/j.ijsolstr.2014.02.025

Eq. (102) should be replaced with

$$\begin{aligned}\psi_1 = & -\left(Xv_{1,1}+\nu Xv_{2,2}+\phi v_{3,1}\right)+\left(\int_0^X x_3 dY-\left\langle\int_0^X x_3 dY\right\rangle\right)(v_{3,11}+\nu v_{3,22})\\ & + c_1\left(\int_0^X \frac{1}{\sqrt{a}}dY-\left\langle\int_0^X \frac{1}{\sqrt{a}}dY\right\rangle+\phi\left\langle\frac{\varphi}{\sqrt{a}}\right\rangle\right)\\ & + \frac{12\varepsilon^2}{h^2}c_1\left(\int_0^X \varphi\mathcal{A}dY-\left\langle\int_0^X \varphi\mathcal{A}dY\right\rangle-\phi\left\langle\mathcal{A}\right\rangle\right)\\ & - \varepsilon\left(\frac{\int_0^X\varphi\int_0^Y\sqrt{a}dZdY-\left\langle\int_0^X\varphi\int_0^Y\sqrt{a}dZdY\right\rangle-\phi\left\langle\int_0^X\sqrt{a}dY\right\rangle}{\langle\sqrt{a}\rangle}\right.\\ & \left. -\int_0^X \varphi XdY+\left\langle\int_0^X\varphi XdY\right\rangle\right)(v_{3,11}+\nu v_{3,22}).\end{aligned} \tag{130}$$

4.3 A short cut derivation

The same results can be derived in a more intuitive and straightforward way, starting from the assumption that the shell displacements can be presented in the form:

$$\begin{aligned}u_\alpha(X,x,y) =& v_\alpha(x,y)-x_3(X)v_{3,\alpha}+\varepsilon\psi^*_\alpha(X,x,y)\\ u_3(X,x,y) =& v_3(x,y)+\varepsilon\psi^*_3(X,x,y)\end{aligned} \tag{131}$$

Then the derivation proceeds as follows for shell strains. We have

$$\begin{aligned}\gamma_{11} =& v_{1,1}-x_3v_{3,11}+\psi^{*\prime}_1+\varphi\psi^{*\prime}_3+\varepsilon\left(\psi^*_{1,1}+\varphi\psi^*_{3,1}\right),\\ 2\gamma_{12} =& v_{1,2}+v_{2,1}-2x_3v_{3,12}+\psi^{*\prime}_2+\varepsilon\left(\psi^*_{1,2}+\psi^*_{2,1}+\varphi\psi^*_{3,2}\right),\\ \gamma_{22} =& v_{2,2}-x_3v_{3,22}+\varepsilon\psi^*_{2,2},\\ \rho_{11} =& \frac{1}{\varepsilon}U'_1-\frac{1}{2\varepsilon}(\ln a)'U_1+U_{1,1}=\frac{\sqrt{a}}{\varepsilon}\left(\frac{U_1}{\sqrt{a}}\right)'+U_{1,1},\\ 2\rho_{12} =& U_{1,2}+U_{2,1}+\frac{1}{\varepsilon}U'_2+\frac{\varphi'}{\varepsilon a^{3/2}}\sqrt{a}\theta,\\ \rho_{22} =& U_{2,2},\end{aligned} \tag{132}$$

with

$$U_1 = n_1(v_{1,1}-x_3v_{3,11}+\psi^{*\prime}_1)+n_3\psi^{*\prime}_3+\sqrt{a}v_{3,1}+\varepsilon(n_1\psi^*_{1,1}+n_3\psi^*_{3,1}), \tag{133}$$

$$U_2 = n_1(v_{1,2}-x_3v_{3,12})+n_3v_{3,2}+\varepsilon(n_1\psi^*_{1,2}+n_3\psi^*_{3,2}), \tag{134}$$

and rotation θ,

$$2\sqrt{a}\theta = v_{1,2}-v_{2,1}+2\varphi v_{3,2}-\psi^{*\prime}_2+\varepsilon(\psi^*_{1,2}-\psi^*_{2,1}+\varphi\psi^*_{3,2}).$$

Please cite as: http://dx.doi.org/10.1016/j.ijsolstr.2014.02.025

The extension strains contributing to the leading terms of the extension energy Eq. (58) are

$$
\begin{aligned}
\gamma_{11}^0 =& v_{1,1} - x_3 v_{3,11} + {\psi^*}'_1 + \varphi \psi_3^{*\prime}, \\
2\gamma_{12}^0 =& v_{1,2} + v_{2,1} - 2x_3 v_{3,12} + \psi_2^{*\prime}, \\
\gamma_{22}^0 =& v_{2,2} - x_3 v_{3,22}.
\end{aligned} \tag{135}
$$

The bending strains contributing to the leading terms of the bending energy Eq. (58) are

$$
\begin{aligned}
\rho_{11}^0 =& \frac{\sqrt{a}}{\varepsilon} \left(\psi_3' - \frac{\varphi}{a} \gamma_{11}^0 \right)' + \sqrt{a} v_{3,11}, \\
2\rho_{12}^0 =& 2\sqrt{a} v_{3,12} - \frac{\varphi'}{2\varepsilon a^{3/2}} (2\gamma_{12}^0), \\
\rho_{22}^0 =& \frac{1}{\sqrt{a}} v_{3,22}.
\end{aligned} \tag{136}
$$

These leading strain measures are the same as those in Eqs. (103), (74), (105), and (112) if

$$
\varepsilon \psi_\alpha = \varepsilon \psi_\alpha^* - x_3 v_{3,\alpha} \qquad \varepsilon \psi_3 = \varepsilon \psi_3^* \tag{137}
$$

With these relations, the displacement field in Eq. (131) is also the same as those in Eq. (59). The solution procedure for ψ_i^* is exactly same as the second step in the previous section if the relations in Eq. (137) are plugged into the equations starting from Eq. (113) all the way to Eq. (130).

5 Equivalent plate energy

Now, everything is ready to compute the equivalent plate energy. It is convenient to split the first approximation of the the strain energy in Eq. (65) into three parts. J_1 is associated with energy in Eq. (80), J_2 with energy in Eq. (70), and J_3 with energy

$$
J_3 = \left\langle \mu h \sqrt{a} (1+\nu) (\gamma_{22}^0)^2 + \frac{\mu h^3}{12} \sqrt{a} (1+\nu) (\rho_{22}^0)^2 \right\rangle. \tag{138}
$$

Let us compute J_1 first. Using Eq. (87) and Eq. (88)

$$
J_1 = \left\langle \mu h \sqrt{a} \, (1+\sigma) \left(\frac{c_1}{\sqrt{a}} \right)^2 + \frac{\mu h^3}{12} \sqrt{a} \, (1+\sigma) \left(c_1 \frac{12 x_3}{h^2} + c_4 \right)^2 \right\rangle. \tag{139}
$$

Please cite as: http://dx.doi.org/10.1016/j.ijsolstr.2014.02.025

Substituting Eq. (21) and Eq. (19) into Eq. (139), J_1 becomes,

$$\begin{aligned}J_1 =& \left\langle \mu h \frac{1}{\sqrt{a}} (1+\sigma) \left(\frac{\varepsilon\mathcal{B}(v_{3,11}+\nu v_{3,22}) - (v_{1,1}+\nu v_{2,2})}{\mathcal{C}} \right)^2 \right. \\ & + \frac{\mu h^3}{12}\sqrt{a}\,(1+\sigma) \left(-\frac{(v_{1,1}+\nu v_{2,2})}{\mathcal{C}} \frac{12}{h^2}(x_3 - \varepsilon\mathcal{B}) \right. \\ & \left.\left. + \left(\frac{1}{\langle\sqrt{a}\rangle} + \frac{12\varepsilon\mathcal{B}}{h^2\mathcal{C}}(x_3-\varepsilon\mathcal{B}) \right)(v_{3,11}+\nu v_{3,22}) \right)^2 \right\rangle \\ =& (v_{1,1}+\nu v_{2,2})^2 \mu(1+\sigma)\frac{1}{\mathcal{C}^2}\left(h\left\langle \frac{1}{\sqrt{a}} \right\rangle + \frac{12}{h}\varepsilon^2 \langle\varphi\mathcal{A}\rangle \right) \\ & + (v_{3,11}+\nu v_{3,22})^2 \mu h(1+\sigma)\left(\frac{\varepsilon^2\mathcal{B}^2}{\mathcal{C}^2}\left\langle \frac{1}{\sqrt{a}} \right\rangle + \frac{h^2}{12}\left(\frac{12^2\varepsilon^4\mathcal{B}^2}{h^4\mathcal{C}^2}\langle\varphi\mathcal{A}\rangle + \frac{1}{\langle\sqrt{a}\rangle} \right) \right) \\ & - (v_{1,1}+\nu v_{2,2})(v_{3,11}+\nu v_{3,22})\mu h(1+\sigma)\left(\frac{2\varepsilon\mathcal{B}}{\mathcal{C}^2}\left\langle \frac{1}{\sqrt{a}} \right\rangle + \frac{24\mathcal{B}\varepsilon^3}{h^2\mathcal{C}^2}\langle\varphi\mathcal{A}\rangle \right).\end{aligned} \tag{140}$$

Note

$$\left\langle \sqrt{a}(x_3 - \mathcal{B}\varepsilon)^2 \right\rangle = \left\langle \sqrt{a}x_3^2 \right\rangle - \frac{\langle\sqrt{a}x_3\rangle^2}{\langle\sqrt{a}\rangle} = \varepsilon^2\langle\varphi\mathcal{A}\rangle, \quad \frac{\langle\sqrt{a}(x_3-\varepsilon\mathcal{B})\rangle}{\langle\sqrt{a}\rangle} = 0. \tag{141}$$

Rewriting Eq. (70)

$$J_2 = \frac{\mu h}{2}\left\langle \frac{1}{\sqrt{a}}\left(\left(2\gamma_{12}^0\right)^2 + \frac{h^2}{12}\left(2\sqrt{a}v_{3,12} - \frac{\varphi'}{2\varepsilon a^{3/2}}2\gamma_{12}^0 \right)^2 \right) \right\rangle. \tag{142}$$

Substituting Eq. (113) and Eq. (20) into Eq. (142),

$$\begin{aligned}J_2 =& (v_{1,2}+v_{2,1})^2\left(\frac{\mu h\alpha_1^2}{2}\left\langle \frac{\sqrt{a}}{(1+\frac{\varphi'^2h^2}{48\varepsilon^2a^3})} \right\rangle \right) \\ & + v_{3,12}^2\frac{\mu h}{2}\left\langle \frac{\sqrt{a}h^2}{3} - \frac{1}{\sqrt{a}}\frac{\frac{h^4\varphi'^2}{12^2\varepsilon^2a^2} - a\alpha_2^2}{1+\frac{\varphi'^2h^2}{48\varepsilon^2a^3}} \right\rangle \\ & - (v_{1,2}+v_{2,1})v_{3,12}\mu h\alpha_1\alpha_2\left\langle \frac{\sqrt{a}}{1+\frac{\varphi'^2h^2}{48\varepsilon^2a^3}} \right\rangle.\end{aligned} \tag{143}$$

Substituting γ_{22}^0 in Eq. (135) and ρ_{22}^0 in Eq. (136) into Eq. (138),

$$\begin{aligned}J_3 =& v_{2,2}^2\mu h(1+\nu)\left\langle\sqrt{a}\right\rangle + v_{3,22}^2\mu h(1+\nu)\left(\left\langle \sqrt{a}x_3^2 \right\rangle + \frac{h^2}{12}\left\langle \frac{1}{\sqrt{a}} \right\rangle \right) \\ & - v_{2,2}v_{3,22}2\mu h(1+\nu)\left\langle \sqrt{a}x_3 \right\rangle.\end{aligned} \tag{144}$$

Please cite as: http://dx.doi.org/10.1016/j.ijsolstr.2014.02.025

If we set

$$\begin{aligned} &\epsilon_{xx} = v_{1,1}, \quad \epsilon_{yy} = v_{2,2}, \quad 2\epsilon_{xy} = v_{1,2} + v_{2,1}, \\ &\kappa_{xx} = -v_{3,11}, \quad \kappa_{yy} = -v_{3,22}, \quad \kappa_{xy} = -v_{3,12}, \end{aligned} \tag{145}$$

in

$$J = \frac{1}{2} \begin{Bmatrix} \epsilon_{xx} \\ \epsilon_{yy} \\ 2\epsilon_{xy} \\ \kappa_{xx} \\ \kappa_{yy} \\ 2\kappa_{xy} \end{Bmatrix}^T \begin{bmatrix} A_{11} & A_{12} & 0 & B_{11} & B_{12} & 0 \\ A_{12} & A_{22} & 0 & B_{12} & B_{22} & 0 \\ 0 & 0 & A_{66} & 0 & 0 & B_{66} \\ B_{11} & B_{12} & 0 & D_{11} & D_{12} & 0 \\ B_{12} & B_{22} & 0 & D_{12} & D_{22} & 0 \\ 0 & 0 & B_{66} & 0 & 0 & D_{66} \end{bmatrix} \begin{Bmatrix} \epsilon_{xx} \\ \epsilon_{yy} \\ 2\epsilon_{xy} \\ \kappa_{xx} \\ \kappa_{yy} \\ 2\kappa_{xy} \end{Bmatrix}, \tag{146}$$

We obtain the relations for the equivalent plate stiffnesses as listed in Eq. (15).

6 Recovery relations

The equivalent plate stiffnesses constants can be used as inputs to carry out a plate analysis, either analytically or numerically, to predict the plate displacement field (v_i) and strain field ($\epsilon_{xx}, \epsilon_{yy}, 2\epsilon_{xy}, \kappa_{xx}, \kappa_{yy}, 2\kappa_{xy}$). This information can be used first to recover displacement field in the original corrugated shell using Eq. (59) with ψ_i solved previously in Eq. (130), (117), and (128). Usually it is more critical to know the strain field and moment field within the original corrugated shell which can be obtained from Eq. (135) and Eq. (136) as those given in Eq. (18). The stress resultants can be recovered using the constitutive relation corresponding to the strain energy in Eq. (58), which can be used to further recover the three-dimensional (3D) stresses based on the relations of the starting shell theory and the three-dimensional elasticity theory. Following [46], the 3D strain field can be recovered as

$$\begin{aligned} \Gamma_{\alpha\beta} &= \gamma^0_{\alpha\beta} + y_3 \rho^0_{\alpha\beta}, \qquad \Gamma_{\alpha 3} = 0, \\ \Gamma_{33} &= -\frac{\nu}{1-\nu}\left(\gamma^0_{11} + \gamma^0_{22} + y_3(\rho^0_{11} + \rho^0_{22})\right), \end{aligned} \tag{147}$$

and the 3D stress field can be recovered as

$$\begin{aligned} \sigma_{11} &= \frac{E}{1-\nu^2}(\Gamma_{11} + \nu\Gamma_{22}), \\ \sigma_{22} &= \frac{E}{1-\nu^2}(\Gamma_{22} + \nu\Gamma_{11}), \\ \sigma_{12} &= \frac{E}{2(1+\nu)} 2\Gamma_{12}, \\ \sigma_{33} &= \sigma_{13} = \sigma_{23} = 0. \end{aligned} \tag{148}$$

Please cite as: http://dx.doi.org/10.1016/j.ijsolstr.2014.02.025

with y_3 as the thickness coordinate of the shell along the transverse normal direction.

7 Validation examples

In this section, two shapes of corrugations are studied. One is a sinusoidal corrugation which represents the symmetric case with no coupling effects, and the other is a exponential-sinusoidal corrugation which is an example of the nonsymmetric corrugations thus exhibiting coupling effects. For the sinusoidal corrugated plate, we also analyzed the original structure directly using the finite element analysis software ANSYS. The recovered displacement and strain fields are compared with the present approach.

7.1 Sinusoidal Shape

The mid-surface of sinusoidal shape,

$$\phi(X) = \frac{T}{\varepsilon}\sin(2\pi X), \tag{149}$$

is characterized by one parameter, T, the rise of the corrugation (Fig. 3). From the definition of $\varphi(X)$ (Eq. (6)),

$$\varphi(X) = \frac{2\pi T}{\varepsilon}\cos(2\pi X). \tag{150}$$

For numerical values we choose $\varepsilon = 0.64$ m, $T = 0.11$ m, $h = 0.005$ m and material properties are taken to be $E = 30$ GPa, $\nu = 0.2$, $\rho = 7830$ kg/m^3. Clearly we have $h/\varepsilon \ll 1$.

The equivalent plate stiffnesses obtained using different approaches are listed in Table. 1. VAPAS is a code introduced in [47] for equivalent plate modeling of panels with microstructures starting from the original 3D elasticity theory. Corrugated structures can be considered as a special case of such panels and the results obtained can be used as benchmark for the present study. For the corrugated profile under consideration, $\langle\phi\sqrt{a}\rangle = 0$, and there is no extension-bending coupling. It is seen from Table. 1 that the results obtained by the present approach are very close to those predicted by VAPAS and Xia *et al.* However, the differences between the present approach and the commonly accepted formulas for A_{11}, A_{12} are noticeable. Note, in this table, we used $D_{12} = \nu D_{11}$ from Eq. (10). Formula (13) gives $A_{11} = 39639$ N/m, which is also well off the correct result.

Please cite as: http://dx.doi.org/10.1016/j.ijsolstr.2014.02.025

Table 1
Equivalent plate stiffnesses of sinusoidal corrugation.

	Eqs. (9)(12)	Xia et al.[19]	VAPAS	Present
A_{11} (N/m)	53805	47613	48152	47613
A_{12} (N/m)	10761	9523	9630	9523
A_{22} (N/m)	1.8708×10^8	1.8708×10^8	1.8692×10^8	1.8708×10^8
A_{66} (N/m)	5.0113×10^7	5.0113×10^7	5.0097×10^7	5.0113×10^7
D_{11} (N·m)	261.004	261.004	263.972	261.004
D_{12} (N·m)	52.20	52.20	52.95	52.20
D_{22} (N·m)	1025270	1068260	1022874	1025540
D_{66} (N·m)	162.39	162.39	163.38	162.39

A square sinusoidal corrugated plate with 11 corrugations is subjected to a uniformly distributed load of 50 Pa in ANSYS. Element SURF154 is overlaid onto element SHELL63 of the corrugated area to enforce the load directions. To satisfy simply supported boundary conditions, besides constraining out of plane movements of four edges, the displacements along four edges are under constraint simultaneously. The deflections of the sinusoidal corrugated plate is shown in Fig. 4. The analytical equation of the deflection as an orthotropic plate [48] is in Eq. (151) with D_{11}, D_{12}, D_{66}, D_{22} obtained previously.

$$v_3(x,y) = \frac{16p_0}{\pi^6} \sum_{m=1}^{\infty} \sum_{n=1}^{\infty} \frac{\sin[m\pi x/r] \sin[n\pi y/s]}{mn\left(\frac{D_{11}m^4}{r^4} + 2\frac{(D_{12}+2D_{66})m^2n^2}{r^2s^2} + \frac{D_{22}n^4}{s^4}\right)}. \tag{151}$$

where p_0 is the pressure, r, s the length and width of the whole corrugated plate, m, n the odd number sequence. The local deflections u_3 can be recovered by Eq. (59) and Eq. (128). The local deflections along the center lines of the corrugated plate ($x = 3.52$m) obtained by ANSYS and current approach are shown in Fig. 5. An excellent agreement is achieved.

Furthermore, 3D strain fields can be recovered based on Eq. (147). By choosing $y_3 = h/2,\ 0,\ -h/2$, the top, the middle, and the bottom strain fields of the shell can be obtained and compared with those from ANSYS respectively. Again, we choose the position along the center lines of the corrugated plate ($x = 3.52$m) to compare Γ_{22} and Γ_{33} from ANSYS and current approach, as shown in Fig. 6 and Fig. 7. Again, one can observe from this figures that our theory can correctly predict the local fields within the original corrugated structure.

Please cite as: http://dx.doi.org/10.1016/j.ijsolstr.2014.02.025

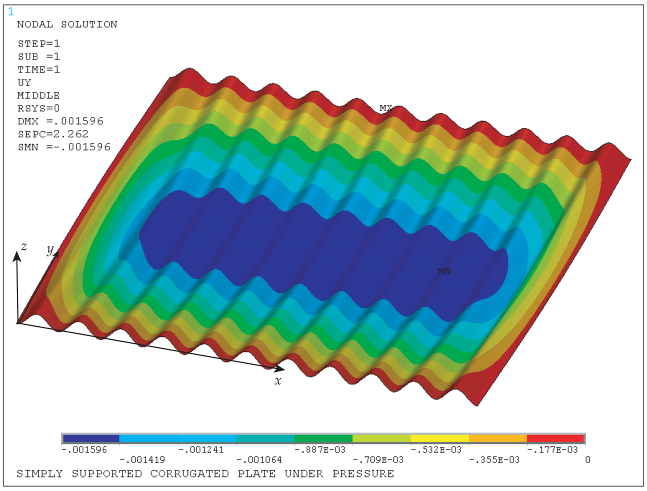

Fig. 4. Deflections of a sinusoidal corrugated plate calculated in ANSYS.

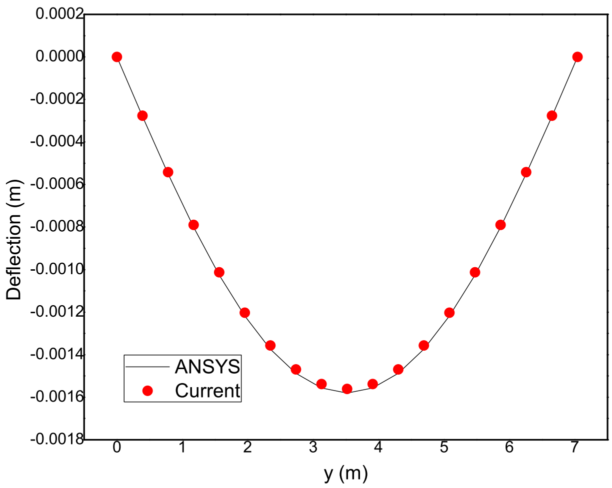

Fig. 5. Deflections along the center line show the good agreement between current approach and ANSYS.

7.2 Exponential-sinusoidal Shape

In the second example, a non-symmetric corrugated shape is chosen to show the coupling effects. We use an exponential-sinusoidal function with unit cell length $\varepsilon = 1$ m,

$$\phi(X) = \eta \left(e^{Sin(2\pi X)} - \left\langle e^{Sin(2\pi X)} \right\rangle \right), \tag{152}$$

as sketched in Fig. 8. An additive constant is added to satisfy Eq. (4). A plot of the dimensionless parameter $B_{22}/(Eh\varepsilon)$ as a function of η is shown

Please cite as: http://dx.doi.org/10.1016/j.ijsolstr.2014.02.025

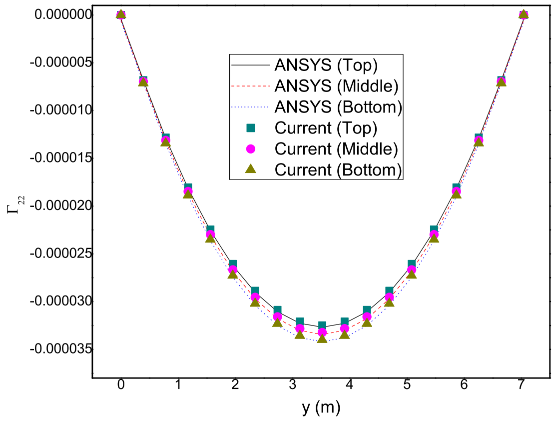

Fig. 6. Comparison of Γ_{22} between ANSYS and current approach.

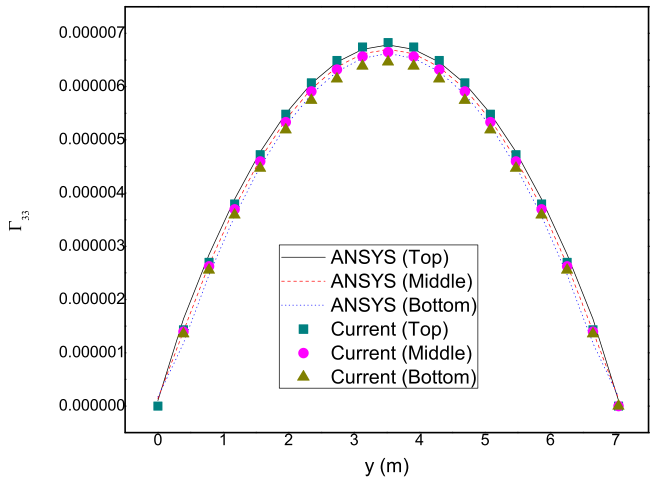

Fig. 7. Comparison of Γ_{33} between ANSYS and current approach..

in Fig. 9. We choose thickness $h = 0.005$ m and material properties $E = 30$ GPa, $\nu = 0.2$. Equivalent plate stiffnesses obtained by different approaches are listed for comparison in Table 2. Since the corrugation is not symmetric, the rise of the corrugation T in Eq. (12) is measured as half of the total swing. Apparently, the extension-bending coupling, particularly the coupling coefficient B_{22} between $v_{2,2}$ and $v_{3,22}$, is not negligible comparing to other stiffnesses terms as η grows larger. For the other stiffness constants, the four sets of results also have noticeable differences for which the present approach, VAPAS and Xia et al. have a better agreement with VAPAS than the results in Eqs. (9)(12) except A_{11} and A_{12}.

Please cite as: http://dx.doi.org/10.1016/j.ijsolstr.2014.02.025

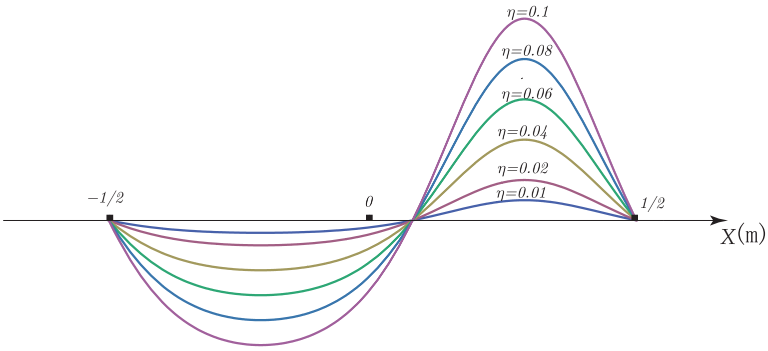

Fig. 8. Shapes of nonsymmetric corrugations for different values of parameter η.

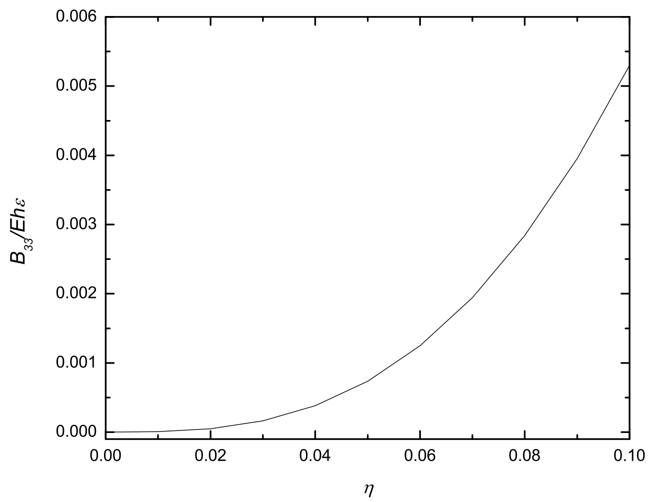

Fig. 9. Coupling coefficient $B_{22}/(Eh\varepsilon)$ as a function of η.

8 Conclusion

The variational asymptotic method has been used to construct an equivalent plate model for corrugated structures. The theory handles general corrugation shape as long as original structure is thin and can be described using the classical shell theory and the length of a single corrugation is small with respect to the characteristic length of macroscopic deformation of the corrugated structure. The present theory not only present a complete set of effective plate stiffnesses but also the complete set of recovery relations to obtain the local fields within the corrugated shell. In comparison to other approaches in the literature for equivalent plate modeling of corrugated structures, the new points of this work are:

(1) The variational asymptotic method of an asymptotic analysis of the strain energy does not invoke any ad hoc assumptions.

Please cite as: http://dx.doi.org/10.1016/j.ijsolstr.2014.02.025

Table 2
Equivalent plate stiffnesses of exponential-sinusoidal corrugation ($\eta = 0.1$).

	Eqs. (9)(12)	Xia et al.[19]	VAPAS	Present
A_{11} (N/m)	47139	43765	46366	43911
A_{12} (N/m)	9427.89	8753.09	9273.22	8782.20
A_{22}(N/m)	1.6759×10^8	1.7088×10^8	1.7072×10^8	1.7088×10^8
A_{66} (N/m)	5.5942×10^7	5.4865×10^7	5.4846×10^7	5.4866×10^7
B_{11} (N)	N/A	N/A	225.98	204.26
B_{12} (N)	N/A	N/A	42.644	40.851
B_{22} (N)	N/A	N/A	817802	794841
D_{11} (N·m)	291.364	285.757	296.106	286.707
D_{12} (N·m)	58.273	57.151	59.679	57.341
D_{22} (N·m)	1.3297×10^6	1.1622×10^6	1.1122×10^6	1.1157×10^6
D_{66} (N·m)	145.47	148.33	153.29	148.33

(2) A complete set of analytical formulas for stiffnesses of the equivalent plate including extension-bending coupling stiffnesses are obtained. These formulas are valid for any corrugated shell with corrugations along one directions.
(3) We presented the complete set of recovery relations for the displacement, strain, and stress fields within the original corrugated shell in terms of the equivalent plate behavior.

The difference of the present approach is demonstrated through a couple of simple examples.

Acknowledgments

This work is financially supported, in part, by the Liebherr-Aerospace company. The views and conclusions contained herein are those of the authors and should not be interpreted as necessarily representing the official policies or endorsement, either expressed or implied, of the sponsor.

References

[1] L. E. Andreeva. *Elastic elements of instruments.* Israel Program for Scientific Translations, 1966.

Please cite as: http://dx.doi.org/10.1016/j.ijsolstr.2014.02.025

[2] D. W. Mccready and D. L. Katz. A study of corrugated fiberboard the effect of adhesive on the strength of corrugated board. Technical report, Deaprtment of Engineering, University of Michigan Ann Arbor, 1939.

[3] E. O. Jr Seaquist. *Bending of rectangular corrugated sandwich plates.* PhD thesis, Iowa State University of Science and Technology, 1964.

[4] G. A. Baum, D. C. Brennan, and C. C. Habeger. Orthotropic elastic constants of paper. *Tappi Journal*, 64:97–101, 1981.

[5] L. A. Carlsson, T. Nordstrand, and B. Westerlind. On the elastic stiffnesses of corrugated core sandwich. *Journal of Sandwich Structures and Materials*, 3:253–267, 2001.

[6] C. C. Liang, M. F. Yang, and P. W. Wu. Optimum design of metallic corrugated core sandwich panels subjected to blast loads. *Ocean Engineering*, 28:825–861, 2001.

[7] J. F. Davalos, P. Z. Qiao, X. F. Xu, J. Robinson, and K. E. Barth. Modeling and characterization of fiber-reinforced plastic honeycomb sandwich panels for highway bridge applications. *Composite Structures*, 52:441 – 452, 2001.

[8] N. Buannic, P. Cartraud, and T. Quesnel. Homogenization of corrugated core sandwich panels. *Composite Structures*, 59:299 – 312, 2003.

[9] Z. Aboura, N. Talbi, S. Allaoui, and M. L. Benzeggagh. Elastic behavior of corrugated cardboard: experiments and modeling. *Composite Structures*, 63:53 – 62, 2004.

[10] N. Talbi, A. Batti, R. Ayad, and Y. Q. Guo. An analytical homogenization model for finite element modelling of corrugated cardboard. *Composite Structures*, 88:280 – 289, 2009.

[11] R. Haj-Ali, J. Choi, B. S. Wei, R. Popil, and M. Schaepe. Refined nonlinear finite element models for corrugated fiberboards. *Composite Structures*, 87:321–333, 2009.

[12] J. Viguié, P. J. Dumont, L. Orgéas, P. Vacher, I. Desloges, and E. Mauret. Surface stress and strain fields on compressed panels of corrugated board boxes. an experimental analysis by using digital image stereocorrelation. *Composite Structures*, 93:2861–2873, 2011.

[13] T. Yokozeki, S. Takeda, T. Ogasawara, and T. Ishikawa. Mechanical properties of corrugated composites for candidate materials of flexible wing structures. *Composites Part A: Applied Science and Manufacturing*, 37:1578–1586, 2006.

[14] C. Gentilinia, L. Nobilea, and K. A. Seffen. Numerical analysis of morphing corrugated plates. *Procedia Engineering*, 1:79–82, 2009.

[15] C. Thill, J. A. Etches, I. P. Bond, K. D. Potter, and P. M. Weaver. Composite corrugated structures for morphing wing skin applications. *Smart Materials and Structures*, 19:124009, 2010.

[16] M. T. Huber. Die theorie des kreuzweise bewehrten eisenbetonplatten. *Der Bauingenieur*, 4:354–360, 1923.

[17] G. Bartolozzi, M. Pierini, U. Orrenius, and N. Baldanzini. An equivalent material formulation for sinusoidal corrugated cores of structural

Please cite as: http://dx.doi.org/10.1016/j.ijsolstr.2014.02.025

sandwich panels. *Composite Structures*, 100:173–185, 2013.

[18] D. Briassoulis. Equivalent orthotropic properties of corrugated sheets. *Computers and Structures*, 23:129–138, 1986.

[19] Y. Xia, M. I. Friswell, and E. I. Saavedra Flores. Equivalent models of corrugated panels. *International Journal of Solids and Structures*, 49(13):1453 – 1462, 2012.

[20] I. V. Andrianov, A. A. Diskovsky, and E. G. Kholod. Homogenization method in the theory of corrugated plates. *Technische Mechanik*, 18:123–133, 1998.

[21] L. I. Manevich, I.V. Andrianov, and V. G. Oshmyan. *Mechanics of periodically heterogeneous structures*. Springer Verlag, 2002.

[22] A. F. Arkhangelskii and V. I. Gorbachev. Effective characteristics of corrugated plates. *Mechanics of Solids*, 42:447–462, 2007.

[23] I. V. Andrianov, J. Awrejcewicz, and A. A. Diskovsky. Asymptotic investigation of corrugated elements with quasi-periodic structures. In *Dynamical Systems - Theory and Applications*, Lodz, Poland, 12 2009.

[24] E. Seydel. Shear buckling of corrugated plates. *Jahrbuch die Deutschen Versuchsanstalt fur Luftfahrt*, 9:233–245, 1931.

[25] R. Szilard. *Theory and analysis of plates*. Prentice-Hall, 1974.

[26] M. S. Troitsky. *Stiffened plates: Bending, stability, and vibrations*. Elsevier, 1976.

[27] D. E. McFarland, B. L. Smith, and W. D. Bernhart. *Analysis of plates*. Spartan Books, 1972.

[28] S. G. Lekhnitskii. Anisotropic plates. Technical report, DTIC Document, 1968.

[29] J. H. Lau. Stiffness of corrugated plate. *Journal of the Engineering Mechanics Division*, 107:271–275, 1981.

[30] C. H. Lee. *Study of corrugated plates*. PhD thesis, University of South Carolina, 1981.

[31] S. Luo and J. C. Suhling. The bending stiffnesses of corrugated board. *Mechanics of Cellulosic Materials*, 145:15–26, 1992.

[32] K. M. Liew, L. X. Peng, and S. Kitipornchai. Buckling analysis of corrugated plates using a mesh-free galerkin method based on the first-order shear deformation theory. *Computational Mechanics*, 38:61–75, 2006.

[33] K. M. Liew, L. X. Peng, and S. Kitipornchai. Vibration analysis of corrugated reissner-mindlin plates using a mesh-free galerkin method. *International Journal of Mechanical Sciences*, 51:642 – 652, 2009.

[34] D. Wennberg, P. Wennhage, and S. Stichel. Orthotropic models of corrugated sheets in finite element analysis. *ISRN Mechanical Engineering*, 2011, 2011.

[35] A. Samanta and M. Mukhopadhyay. Finite element static and dynamic analyses of folded plates. *Engineering Structures*, 21:277 – 287, 1999.

[36] J. T. Easley and E. D. McFarland. Buckling of light gage corrugated metal shear diaphragms. *Journal of the Structural Division*, 95:1497–1516, 1969.

Please cite as: http://dx.doi.org/10.1016/j.ijsolstr.2014.02.025

[37] J. T. Easley. Buckling formulas for corrugated metal shear diaphragms. *Journal of the Structural Division*, 101:1403–1417, 1975.

[38] M. N. EI-Atrouzy. Structural properties of corrugated sheets used in cylindrical shells. Master's thesis, The University of Windsor, 1969.

[39] G. Abdel-Sayed. Critical shear loading of curved panels of corrugated sheets. *Journal of the Engineering Mechanics Division*, 96:895–912, 1970.

[40] O. A. Marzouk and G. Abdel-Sayed. Linear theory of orthotropic cylindrical shells. *Journal of the Structural Division*, 99:2287–2306, 1973.

[41] J. M. Davies. Calculation of steel diaphragm behavior. *Journal of the Structural Division*, 102:1411–1430, 1976.

[42] M. N. El-Atrouzy and G. Abdel-Sayed. Prebuckling analysis of orthotropic barrel-shells. *Journal of the Structural Division*, 104:1775–1786, 1978.

[43] N. S. Bakhvalov. Average characteristics of bodies with periodic structure. *Soviet Mathematics*, 218:1046–1048, 1974.

[44] N. S. Bakhvalov and G. Panasenko. *Homogenisation: Averaging Processes in Periodic Media*. Kluwer-Academic Publishers Group, Norwell, MA/Dordrecht, 1989.

[45] V. L. Berdichevsky. *Variational Principles of Continuum Mechanics: II. Applications*. Springer Verlag, 2009.

[46] W. Yu, D. H. Hodges, and V. V. Volovoi. Asymptotic generalization of Reissner-Mindlin theory: accurate three-dimensional recovery for composite shells. *Computer Methods in Applied Mechanics and Engineering*, 191(44):5087 – 5109, Oct. 2002.

[47] C. Y. Lee and W. Yu. Homogenization and dimensional reduction of composite plates with in-plane heterogeneity. *International Journal of Solids and Structures*, 48:1474–1484, 2011.

[48] J. N. Reddy. *Theory and Analysis of Elastic Plates and Shells*. CRC Press, Boca Raton, 2007.

Please cite as: http://dx.doi.org/10.1016/j.ijsolstr.2014.02.025